# Methylene-Bridged Metallocenes with 2,2′-Methylenebis[1*H*-inden-1-yl] Ligands: Synthesis, Characterization, and Polymerization Catalysis of a Synthetically Simple Class of $C_2$- and $C_{2v}$-Symmetric *ansa*-Metallocenes

by **Luigi Resconi***[a]), **Isabella Camurati**[a]), **Cristina Fiori**[a]), **Davide Balboni**[a]), **Pierluigi Mercandelli***[b]), and **Angelo Sironi**[b])

[a]) Basell Polyolefins, Centro Ricerche G. Natta, I-44100 Ferrara
(e-mail: luigi.resconi@basell.com)
[b]) Dipartimento di Chimica Strutturale, Università di Milano, via Venezian 21, I-20133 Milano
(e-mail: pierluigi.mercandelli@unimi.it)

Dedicated to Professor *Giambattista Consiglio* on the occasion of his 65th birthday

The acid-catalyzed reaction between formaldehyde and 1*H*-indene, 3-alkyl- and 3-aryl-1*H*-indenes, and six-membered-ring substituted 1*H*-indenes, with the 1*H*-indene/$CH_2O$ ratio of 2 : 1, at temperatures above 60° in hydrocarbon solvents, yields 2,2′-methylenebis[1*H*-indenes] **1**–**8** in 50–100% yield. These 2,2′-methylenebis[1*H*-indenes] are easily deprotonated by 2 equiv. of BuLi or MeLi to yield the corresponding dilithium salts, which are efficiently converted into *ansa*-metallocenes of Zr and Hf. The unsubstituted dichloro{(1,1′,2,2′,3,3′,3a,3′a,7a,7′a-$\eta$)-2,2′-methylenebis[1*H*-inden-1-yl]}zirconium ([$ZrCl_2$(**1′**)]) is the least soluble in organic solvents. Substitution of the 1*H*-indenyl moieties by hydrocarbyl substituents increases the hydrocarbon solubility of the complexes, and the presence of a substituent larger than a Me group at the 1,1′ positions of the ligand imparts a high diastereoselectivity to the metallation step, since only the racemic isomers are obtained. Methylene-bridged '*ansa*-zirconocenes' show a noticeable open arrangement of the bis[1*H*-inden-1-yl] moiety, as measured by the angle between the planes defined by the two $\pi$-ligands (the 'bite angle'). In particular, of the 'zirconocenes' structurally characterized so far, the dichloro{(1,1′,2,2′,3,3′,3a,3′a,7a,7′a-$\eta$)-2,2′-methylenebis[4,7-dimethyl-1*H*-inden-1-yl]}zirconium ([$ZrCl_2$(**5′**)] is the most open. The mixture [$ZrCl_2$(**1′**)]/methylalumoxane (MAO) is inactive in the polymerization of both ethylene and propylene, while the metallocenes with substituted indenyl ligands polymerize propylene to atactic polypropylene of a molecular mass that depends on the size of the alkyl or aryl groups at the 1,1′ positions of the ligand. Ethene is polymerized by *rac*-dichloro-{(1,1′,2,2′,3,3′,3a,3′a,7a,7′a-$\eta$)-2,2′-methylenebis[1-methyl-1*H*-inden-1-yl]}zirconium ([$ZrCl_2$(**2′**)])/MAO to polyethylene waxes (average degree of polymerization *ca.* 100), which are terminated almost exclusively by ethenyl end groups. Polyethylene with a high molecular mass could be obtained by increasing the size of the 1-alkyl substituent.

**Introduction.** – A large body of literature exists on the chemistry and catalytic properties of bridged geometrically rigid metallocenes (also referred to as *ansa*-metallocenes) having ligands based on two (variably substituted) 1*H*-inden-1-yl moieties, bridged *via* the 1,1′ positions of the bis[1*H*-inden-1-yl] ligands (*Fig. 1*) [1]. Since the two indenyl moieties have two enantiotopic faces, these metallocenes are usually obtained as mixtures of their racemic and *meso* isomers (*Scheme 1*), and several protocols have been developed for increasing the diastereoselectivity of the metallation step [2].

© 2006 Verlag Helvetica Chimica Acta AG, Zürich

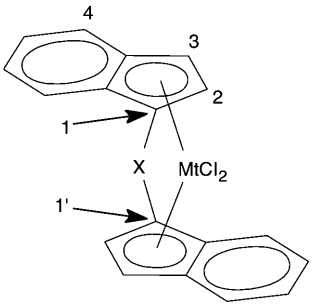


Fig. 1. *General structure of a* $C_2$*-symmetric* ansa*-metallocene with a 1,1′-linked bis[1*H*-inden-1-yl] ligand*

*Scheme 1*

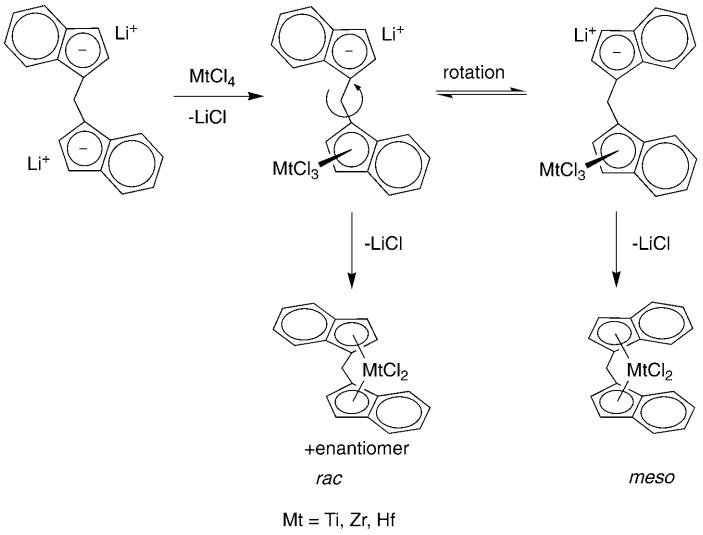


On the other hand, several examples of the synthetically more challenging *ansa*-metallocenes with indenyl ligands bridged through their 2,2′ positions have been reported (*Fig. 2*) [3–5], and one structurally related system with a substituted tetrahydroindenyl system having homotopic faces has also been reported in the literature [6].

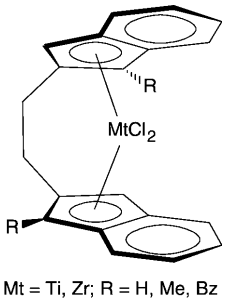


Fig. 2. *General structure of* ansa*-metallocenes with a 2,2′-(ethane-1,2-diyl)-bis[1*H*-inden-1-yl] ligand*

While ligands of this type can in principle give rise to both racemic and *meso* 'zirconocene' isomers when R≠H (*Scheme 2*), both isomers are expected to be aspecific in propylene polymerization based on local symmetry considerations and nonbonded-interactions analysis (*Corradini*'s model for enantioface selectivity in enantiomorphic-site-controlled chain growth) [7].

*Scheme 2*

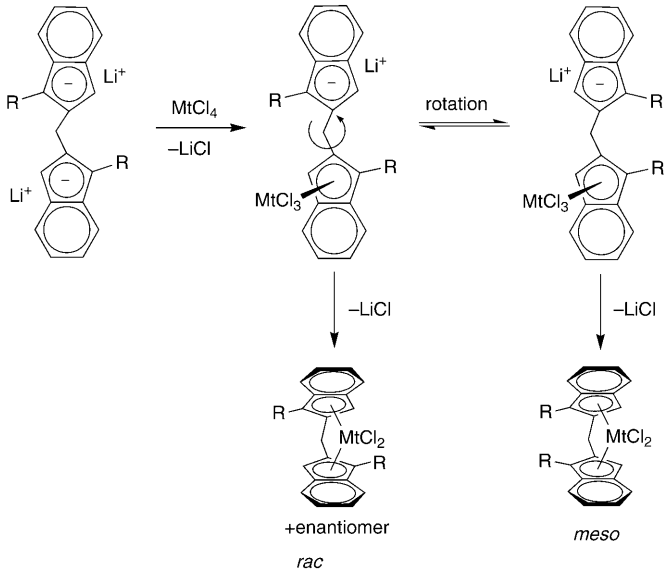


When R = H, the two unsubstituted coordinating indenyl moieties are homotopic and thus can produce one compound only upon metallation. Such an achiral (thus aspecific) 'zirconocene', [$ZrCl_2${2,2′-$CH_2CH_2$(1*H*-indenyl)$_2$}], if active, would produce atactic polypropylene. This ligand design has been exploited by *Nantz*, who described the synthesis of a series of 'titanocenes' and 'zirconocenes' of this type (*Fig. 3*) [3–5] but their catalytic behavior in olefin polymerization was not investigated. *Nantz* and coworkers devised two synthetic strategies for the synthesis of the 2,2′-ethanediylbis[1*H*-indene] ligand precursors (*Schemes 3* and *4*) [3][8].

*Scheme 3*. From [3].

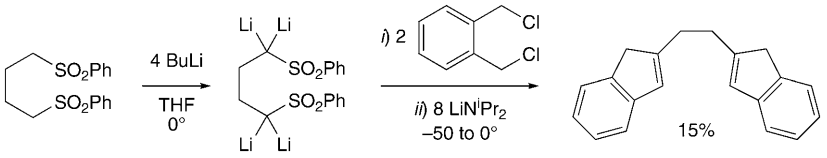


*Schaverien* and co-workers have improved the synthesis of the 2,2′-(ethane-1,2-diyl)bis[1*H*-inden-1-yl] ligand precursors (*Scheme 5*), and have shown that the corresponding ethanediyl-bridged 'zirconocenes' produce very low molecular mass atactic polypropylenes (PP), and require $H_2$ for their activation [9].

*Scheme 4*. From [5] and [8].

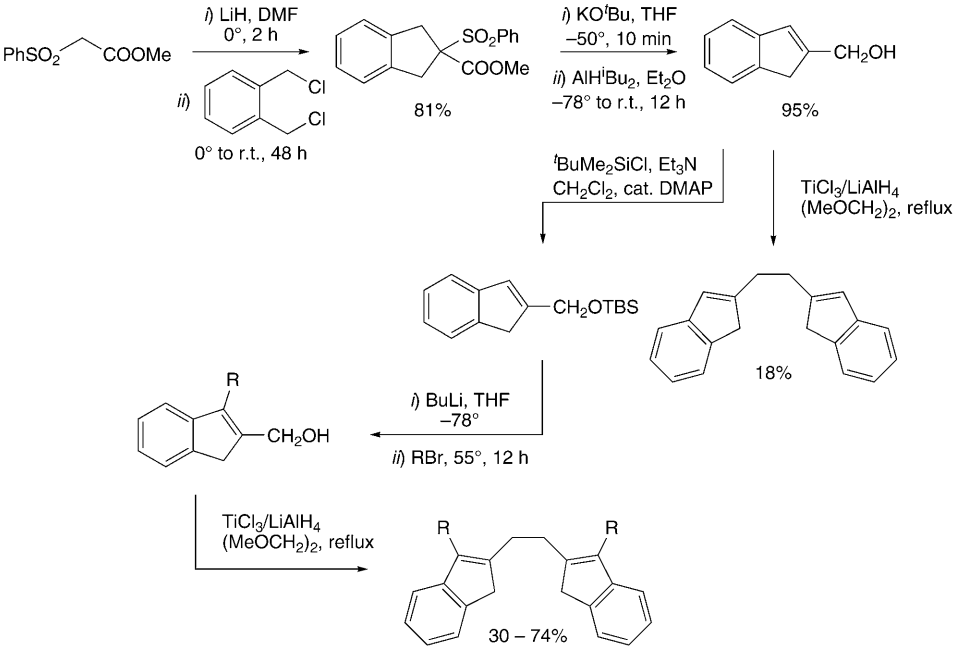


*DSM* researchers have reported the synthesis of a series of 2,2′-linked bis[1*H*-inden-1-yl] systems, including the S-bridged [$ZrCl_2${2,2′-S(1*H*-inden-1-yl)$_2$}] and [$ZrCl_2${2,2′-S(1-Bn-1*H*-inden-1-yl)$_2$}] and the $CH_2$-bridged [$ZrCl_2${2,2′-$CH_2$(1*H*-inden-1-yl)$_2$}] complexes [10]. The metallocenes so far described in the above references are shown in *Fig. 3*.

While the syntheses of both dimethyldi(1*H*-inden-2-yl)silane and di(1*H*-inden-2-yl) sulfide are relatively simple [10], the synthesis of 2,2′-methylenebis[1*H*-indene] is quite laborious. The syntheses of 2,2′-methylenebis[1*H*-indene] (**1**) by the *DSM* group [10] and *Schaverien* and co-workers [9] are shown in *Schemes 6* and *7*, respectively.

*Idemitsu* described the synthesis of 2,2′-(1-methylethylidene)bis[1*H*-indene] ligand precursors (*Scheme 8*), which were then used in the synthesis of doubly bridged complexes [11]. An alternative synthetic protocol for related ligands has been described by *Herzog* and co-workers [12].

All the above methods are multistep and result in low overall yields. We discovered that the acid-catalyzed reaction between 1*H*-indenes and formaldehyde (a modified *Prins*-type condensation) provides a direct, selective, and atom-economical synthesis of 2,2′-methylenebis[1*H*-indenes] (*Scheme 9*) [13].

Here we describe this simple, one-step synthesis of the symmetric 2,2′-methylenebis[1*H*-indene] ligand precursors **1**–**5**, the synthesis of their alkyl and silyl derivatives **6**–**8**, and the synthesis, characterization and evaluation in ethylene and propylene pol-

*Scheme 5*. From [9].

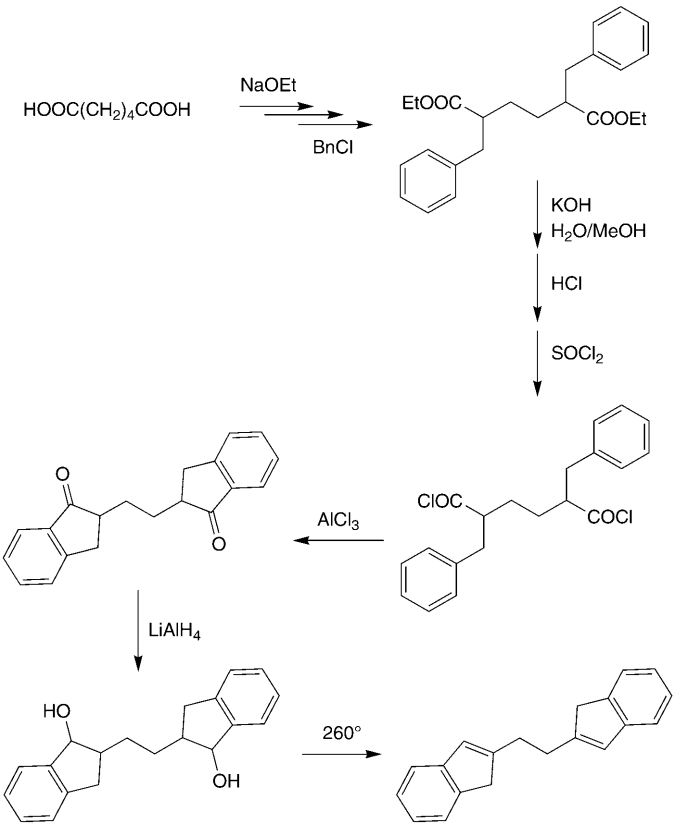


Scheme 6. *Synthesis of 2,2′-Methylenebis[1*H*-indene]* (**1**) *According to* [10]

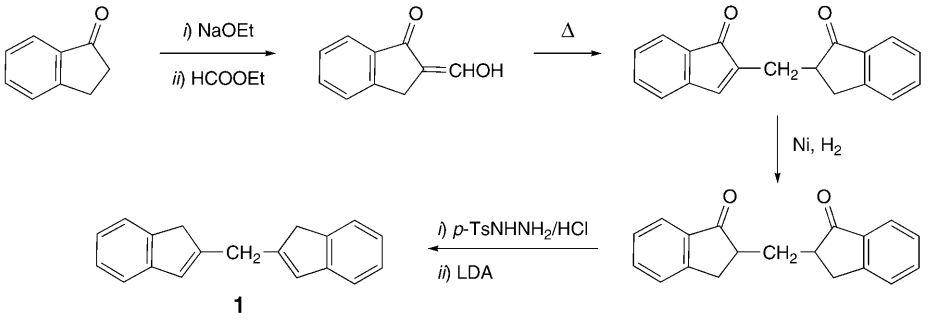


**1**

LDA = lithium diisopropylamide

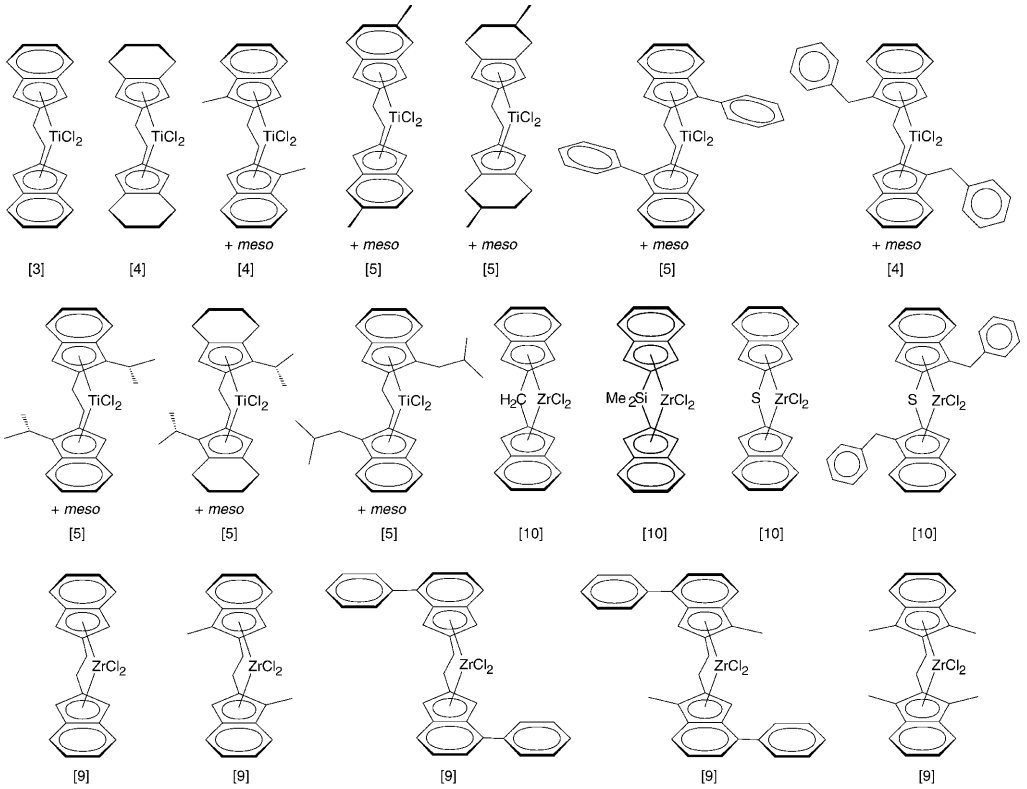


Fig. 3. *Known examples of* ansa-*metallocenes with 2,2′-linked bis[1*H*-inden-1-yl] ligands*

Scheme 7. *Synthesis of 2,2′-Methylenebis[1*H*-indene]* (**1**) *According to* [9]

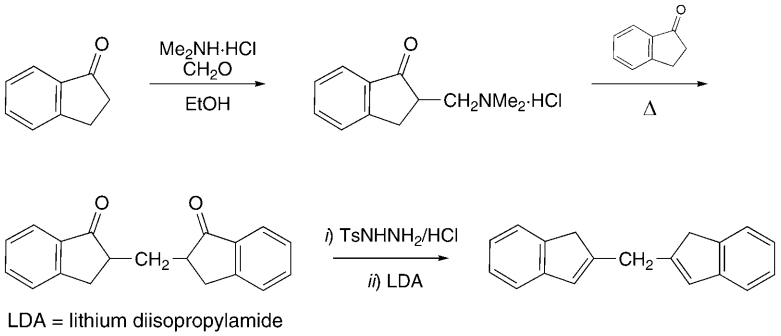


ymerization of the corresponding 'dichlorozirconocenes' [$ZrCl_2$(**1′**)][1]) to [$ZrCl_2$(**8′**)][1]), and the 'dimethylmetallocenes' *rac*-[$ZrMe_2$(**2′**)][1]) and *rac*-[$HfMe_2$(**4′**)][1]) (*Fig. 4*).

---

[1]) For convenience, only one enantiomer of the *rac* isomer is depicted; for the *rac*/*meso* ratios, see *Exper. Part*. The ligands **1′**–**8′** are the dianions of the precursors **1**–**8**.

*Scheme 8.* From [11].

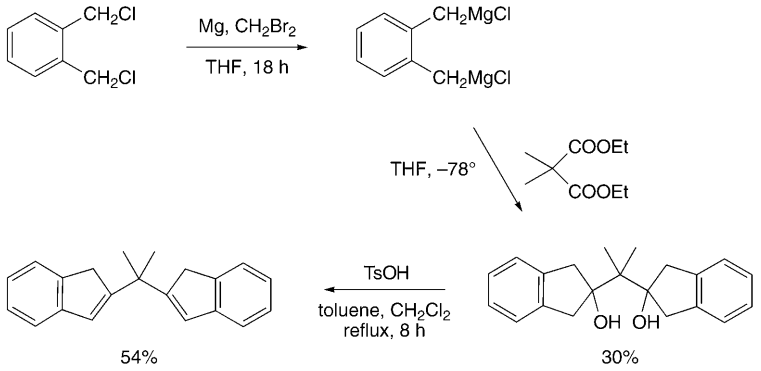


Scheme 9. *One-Step Synthesis of 2,2′-Methylenebis[1*H*-indenes].* R = H, Me, Ph, $^t$Bu, etc.

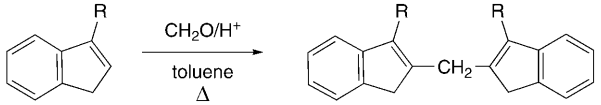


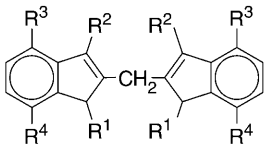


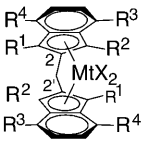


**1** $R^1 = R^2 = R^3 = R^4 = H$
**2** $R^2 = Me$, $R^1 = R^3 = R^4 = H$
**3** $R^2 = Ph$, $R^1 = R^3 = R^4 = H$
**4** $R^2 = {}^t\text{Bu}$, $R^1 = R^3 = R^4 = H$
**5** $R^3 = R^4 = Me$, $R^1 = R^2 = H$
**6** $R^2 = PhCH_2$, $R^1 = R^3 = R^4 = H$
**7** $R^1 = Me_3Si$, $R^2 = R^3 = R^4 = H$
**8** $R^1 = Me_3Si$, $R^2 = Me$, $R^3 = R^4 = H$

$[ZrCl_2(\mathbf{1'})]^1)$ X = Cl, $R^1 = R^2 = R^3 = R^4 = H$
$[ZrCl_2(\mathbf{2'})]^1)$ X = Cl, $R^1 = Me$, $R^2 = R^3 = R^4 = H$
$[ZrMe_2(\mathbf{2'})]^1)$ X = Me, $R^1 = Me$, $R^2 = R^3 = R^4 = H$
$[ZrCl_2(\mathbf{3'})]^1)$ X = Cl, $R^1 = Ph$, $R^2 = R^3 = R^4 = H$
$[ZrCl_2(\mathbf{4'})]^1)$ X = Cl, $R^1 = {}^t\text{Bu}$, $R^2 = R^3 = R^4 = H$
$[HfMe_2(\mathbf{4'})]^1)$ X = Me, $R^1 = {}^t\text{Bu}$, $R^2 = R^3 = R^4 = H$
$[ZrCl_2(\mathbf{5'})]^1)$ X = Cl, $R^3 = R^4 = Me$, $R^1 = R^2 = H$
$[ZrCl_2(\mathbf{6'})]^1)$ X = Cl, $R^1 = PhCH_2$, $R^2 = R^3 = R^4 = H$
$[ZrCl_2(\mathbf{7'})]^1)$ X = Cl, $R^1 = Me_3Si$, $R^2 = R^3 = R^4 = H$
$[ZrCl_2(\mathbf{8'})]^1)$ X = Cl, $R^1 = Me$, $R^2 = Me_3Si$, $R^3 = R^4 = H$

Fig. 4. *Ligands and metallocenes described in the present work*

**Results and Discussion.** – 1. *Surprises from an Old Reaction, the* Prins *Condensation of 1*H*-Indene with Formaldehyde Reinvestigated: Synthesis of the 2,2′-Methylenebis[1*H*-inden-1-yl) Ligand Precursors.* The acid-catalyzed dimerization of 1*H*-indenes (toluene, TsOH, 80°) is known to give 2-(indan-1-yl)-1*H*-indene, likely due to the stability of the intermediate benzylic cation (*Scheme 10*). The acid-catalyzed condensation of aldehydes and olefins, the *Prins* reaction (*Scheme 11*), produces allylic alcohols and 1,3-dioxanes [14].

When applied to 1*H*-indene and excess formaldehyde, the *Prins* reaction was shown to produce 4,4a,5,9b-tetrahydroindeno[1,2-*d*]-1,3-dioxane (**9**) [15], and it would be expected to produce also 1*H*-indene-2-methanol (**10**). We discovered that the structure of the formed product is highly dependent on the reactant ratio (*Scheme 12*) [13]. *Path*

*Scheme 10*

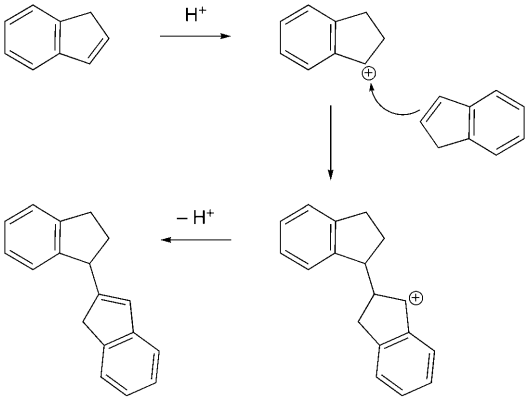


*Scheme 11*

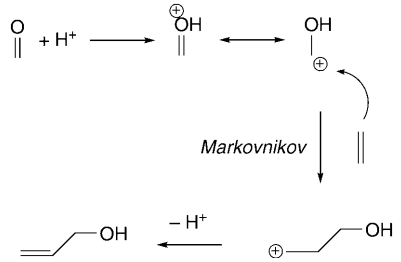


Scheme 12. *The* Prins *Condensation of $CH_2O$ with 1*H*-Indene: Influence of the 1*H*-Indene/$CH_2O$ Ratio*

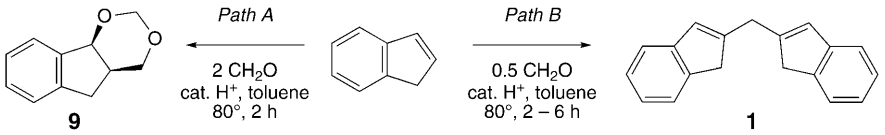


*B* provides the first direct protocol for 2,2′-methylenebis[1*H*-indene] (**1**) and related 2,2′-linked bis[1*H*-indene] ligand precursors.

The mechanisms for the two reactions *A* and *B* are supposed to be strictly related (*Scheme 13*). The intermediate 1*H*-indene-2-methanol (**10**) [8] was observed as a minor product by gas chromatography of the reaction mixtures but could not be isolated in pure form.

The experimental results of this modified *Prins* condensation of 1*H*-indene and several substituted 1*H*-indenes are shown in *Table 1*. Remarkably, no product was observed on condensation of 1-methyl-1*H*-indene and 1-(*tert*-butyl)-1*H*-indene [16], which needed to be isomerized (under basic conditions) to their respective 3-alkyl-1*H*-indene isomers prior to coupling.

*Scheme 13*

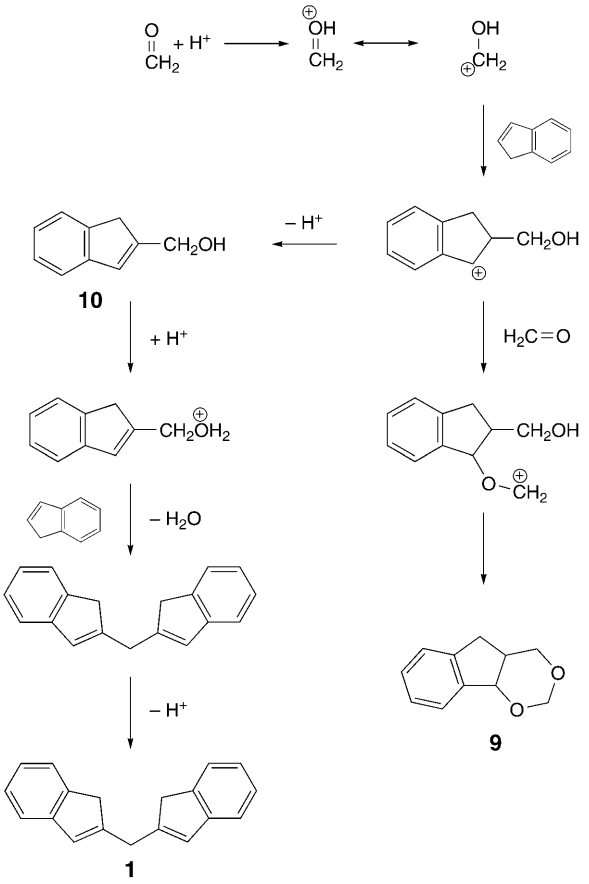


Virtually any source of $CH_2O$ can be used in the modified *Prins* condensation although formaline gave better results compared to trioxane and paraformaldehyde. Given the toxicity of $CH_2O$, we found the use of 1,3-dioxolane as a source of monomeric formaldehyde particularly convenient. This reagent is nontoxic and readily available, and is more conveniently used in excess with respect to the 1*H*-indene substrate. In addition, we found that 1,3-dioxolane gives similar yields of the final 2,2′-methylenebis[1*H*-indenes] as with formaline (*Scheme 14*).

Scheme 14. *Synthesis of 2,2′-Methylenebis[1*H*-indenes] from 1*H*-Indenes and 1,3-Dioxolane.* R = H, 50% of **1**; R = $^t$Bu, 84% of **4**.

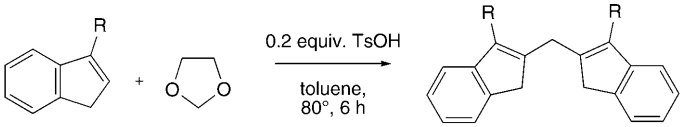

Table 1. *Formaldehyde/1*H-*Indene Condensation Catalyzed by TsOH in Toluene at 80°*[a])

| | 1*H*-Indene/$CH_2O$ ratio | $H^+$/1*H*-Indene ratio | Reaction time [h] | Unreacted 1*H*-indene[b]) | 1*H*-Indene/$CH_2OH$[b]) ratio | Product | Conversion[b]) | Purity[b]) | Isolated yield [%] |
|---|---|---|---|---|---|---|---|---|---|
| 1*H*-Indene | 2.00 | 0.10 | 2 | 25.1 | | **1** | 53.5 | | |
| 1*H*-Indene | 2.01 | 0.20 | 2 | 11.6 | | **1** | 67 | | |
| 1*H*-Indene | 2.01 | 0.20 | 2 | 12.7 | | **1** | 49.3 | | |
| 1*H*-Indene | 2.01 | 0.20 | 6 | 20.5 | 3.4 | **1** | 56.4 | | |
| 1*H*-Indene | 1.51 | 0.20 | 1 | 7.1 | | **1** | 65.8 | | |
| 1*H*-Indene | 1.00 | 0.20 | 1 | 1.8 | 6 | **1** | 59.6 | | |
| 1*H*-Indene | 0.50 | 0.20 | 5 min | 36.6 | 45.7 | **1** | 4.2 | | |
| 1*H*-Indene | 2.01 | 0.20 | 6 | 20 | | **1** | 59 | | |
| 3-Methyl-1*H*-indene | 1.49 | 0.20 | 1 | 0.4 | | **2** | 85.9 | 89.8 | 89.84 |
| 3-Phenyl-1*H*-indene | 1.99 | 0.20 | 6 | n.d. | n.d. | **3** | n.d. | 97.3 | 95.20 |
| 3-(*tert*-Butyl)-1*H*-indene | 1.51 | 0.20 | 6 | 8.9 | | **4** | 79.5 | 90.9 | 76.81 |
| 4,7-Dimethyl-1*H*-indene | 2.00 | 0.20 | 3 | 14.8 | | **5** | 82.4 | 90.2 | 44.16 |

[a]) Formaline (37% in $H_2O$). [b]) By GC, % peak area.

Although 3,3′-dialkyl-substituted 2,2′-methylenebis[1*H*-indenes] can be prepared in two ways (*Scheme 15*), the condensation reaction is more efficient when starting from the 3-substituted indene. Nevertheless, by reaction of **1** with two equiv. of BuLi, followed by excess RCl, we obtained in good to high yield 2,2′-methylenebis[3-methyl-1*H*-indene] (**2**), 2,2′-methylenebis[3-benzyl-1*H*-indene] (**6**), and 2,2′-methylenebis[1-(trimethylsilyl)-1*H*-indene] (**7**), while 2,2′-methylenebis[1-(trimethylsilyl)-3-methyl-1*H*-indene] (**8**) was obtained from the dilithium salt of **2** and excess $Me_3SiCl$.

Scheme 15. *Two Alternative Syntheses of 2,2′-Methylenebis[3-methyl-1*H*-indene]* (**2**)

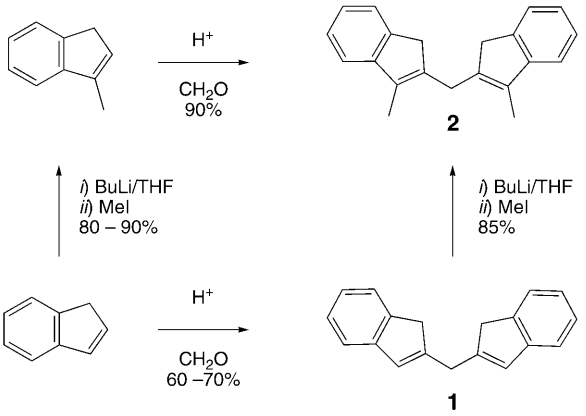


This modified *Prins* condensation reaction is highly regioselective, and the regiochemistry *can not* be reversed, as shown by the reaction with 2-methyl-1*H*-indene, which gives only the 1,3-dioxane **11** (*Scheme 16*).

*Scheme 16*

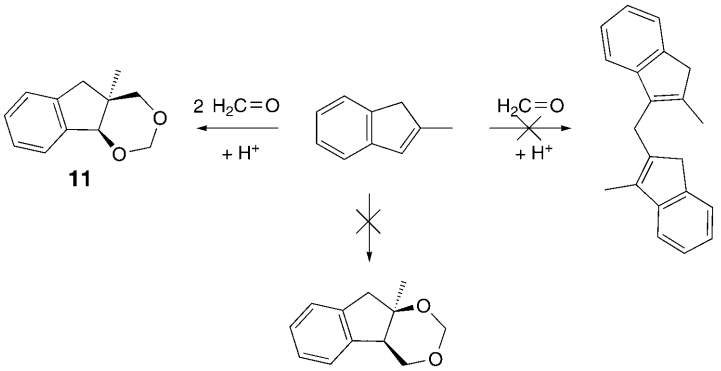


The scope of the modified *Prins* condensation seems to be limited to formaldehyde. Benzaldehyde gives a complicated mixture of products containing only 10% of the product with the correct mass for 2,2′-benzylidenebis[1*H*-indene], and ketones ($Me_2$-CO or $Ph_2CO$) do not react under the conditions employed for $CH_2O$ since the only product observed is the 1*H*-indene dimer.

2. *Synthesis of the 'Zirconocenes'.* The 2,2′-methylenebis[1*H*-indenes] **1**–**8** are easily and efficiently converted into the corresponding methylene-bridged metallocenes (yields 60–100%) by reacting the dilithium salt of the bis[1*H*-indene] with $MtCl_4$ in $Et_2O$/toluene. The *rac*/*meso* selectivity is a function of the size of the hydrocarbyl substituent at the indene moieties. For example, [$ZrCl_2$(**2′**)] ($R^1$ = Me) was obtained as a *rac*/*meso* 2:1 mixture (from which the pure *rac* isomer was separated by extraction in $CH_2Cl_2$), while only the *rac* isomer of [$ZrCl_2$(**4′**)] ($R^1$ = $^t$Bu) was formed (*Scheme 17*). Also for this class of ligands, the dimethyl metallocenes [$MtMe_2$(L)] (Mt = Zr, L = **2′**; Mt = Hf, L = **4′**) can be efficiently obtained by direct synthesis [17]. The metallocenes prepared are shown in *Fig. 5*.

Scheme 17. *Synthesis of Dichloro{1,1′,2,2′,3,3′,3a,3′a,7a,7′a-η)-2,2′-methylenebis[1-methyl-1*H*-inden-1-yl]}zirconium* [$ZrCl_2$(**2′**)]

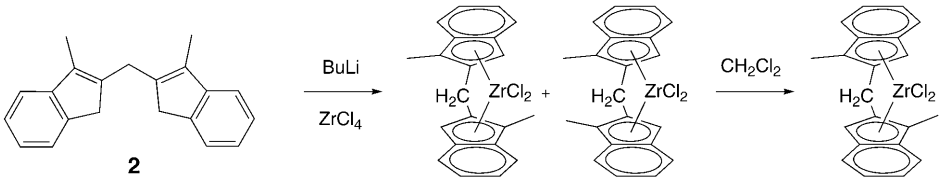


**2**

*rac*/*meso* 2:1

[$ZrCl_2$(**2′**)]

3. *Crystal and Molecular Structures.* The molecular structures of the 1,1′-di(*tert*-butyl), 1,1′-bis(trimethylsilyl), and 4,4′,7,7′-tetramethyl derivatives [$ZrCl_2$(**4′**)], [$ZrCl_2$(**7′**)], and [$ZrCl_2$(**5′**)], respectively, were determined by X-ray diffraction analysis. *Fig. 6* shows frontal ORTEP views of the three molecules, with a partial labeling Scheme. *Table 2* contains the most relevant bonding parameters for the three compounds. *Table 3* contains the angles between some relevant least-squares planes, a few slip-fold indicators, and the values of the geometric parameters described in *Fig. 7*.

The three compounds are isostructural and crystallize in the monoclinic space group *C*2/*c* with a crystallographically imposed two-fold symmetry, the molecules lying about the *Wycoff* position 4*e*. Differences in cell parameters and volumes can easily be explained by taking into account the growing intrinsic volume demands made by the Me, the $^t$Bu, and the $Me_3Si$ substituents in [$ZrCl_2$(**5′**)], [$ZrCl_2$(**4′**)], and [$ZrCl_2$(**7′**)], respectively. In these compounds the metal atom is pseudotetrahedrally coordinated by the two cyclopentadienyl groups of the bis[1*H*-indenyl] moiety and the two chloro ligands. As usual for bent metallocenes, the overall coordination environment is best described by the set of parameters depicted in *Fig. 7*, which can be related to the accessibility of the Zr-atom. In particular, the smaller the 'bite angle' $\beta$ and the bigger the cp–Zr–cp′ angle $\alpha$, the more the metal is tucked into the ligand envelope. As previously stated [18], these parameters are very sensitive to differences in the number and type of the *ansa* atoms, while the presence of substituents on the ligand leads to only minor changes in the *local* geometry around the metal atom.

Only two (2,2′-*ansa*-bis[1*H*-indenyl])dichlorozirconium complexes have been structurally characterized so far, namely the *cis*-1,2-dicyclohexylcyclobutane-1,2-diyl [19]

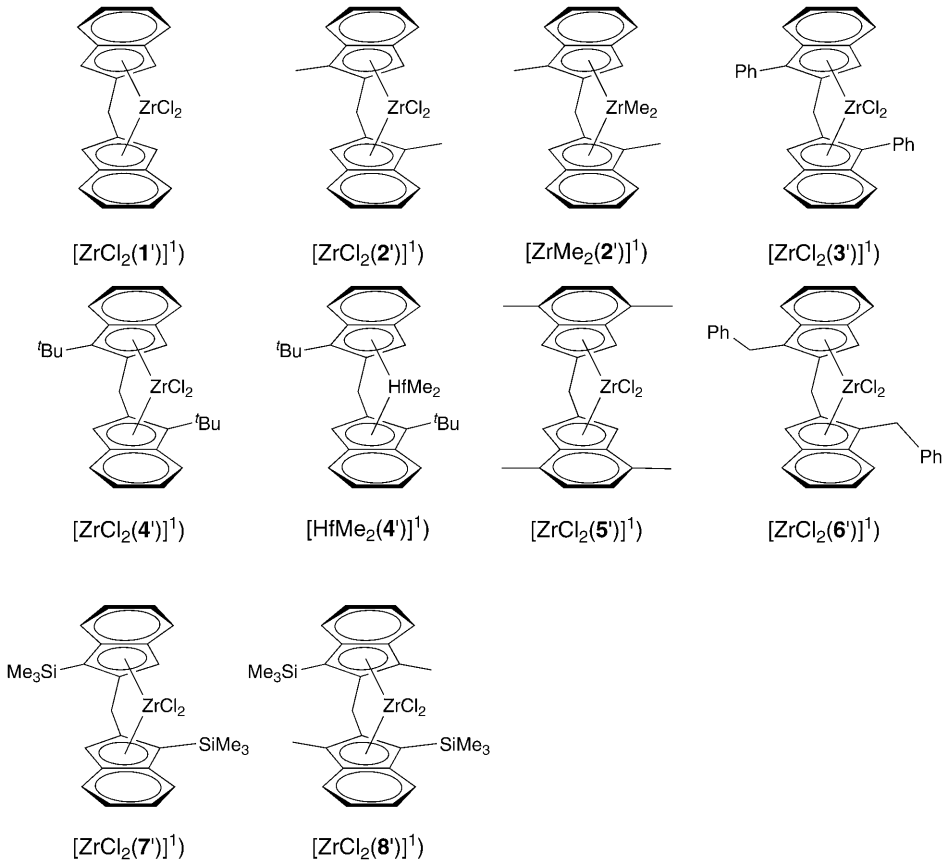


Fig. 5. *Metallocenes synthesized and tested in this work*

and the 1,1′-[biphenyl]-2,2′-diyl [20] derivatives. The bite angles found in these compounds (61.4 and 55.8°, resp.) are noticeably smaller than the angles found in the $CH_2$-bridged complexes [$ZrCl_2$(**4′**)], [$ZrCl_2$(**7′**)], and [$ZrCl_2$(**5′**)], in agreement with the presence of longer *ansa* bridges (two- and four-atoms long, resp.).

As far as '*ansa*-zirconocenes' with single-atom linkers are concerned, a survey of the *Cambridge Structural Database* [21] shows that the widespread dimethylsilylene ($Me_2Si<$) bridged derivatives, due to the larger covalent radius of the Si-atom, present a small bite angle (57.8–64.3°), followed by the isopropylidene ($Me_2C<$) and the diphenylmethylene ($Ph_2C<$) bridged derivatives (70.6–73.9° and 70.6–74.1°, resp.). The $CH_2$-bridged derivatives show the largest bite angle values (up to 76.4°). Data reported in *Table 3* for the three $CH_2$-bridged complexes [$ZrCl_2$(**4′**)], [$ZrCl_2$(**7′**)], and [$ZrCl_2$(**5′**)] confirm this behavior. Indeed, the 4,4′,7,7′-tetramethyl derivative [$ZrCl_2$(**5′**)] is the most open 'zirconocene' structurally characterized so far. The great accessibility of the Zr-atom in this complex is highlighted in *Fig. 8*, in which [$ZrCl_2$(**5′**)] ('bite angle' 76.9°) is compared to its 1*H*-inden-1-yl analog [$ZrCl_2${*rac*-1,1′-$CH_2$(4,7-$Me_2$-1*H*-inden-1-

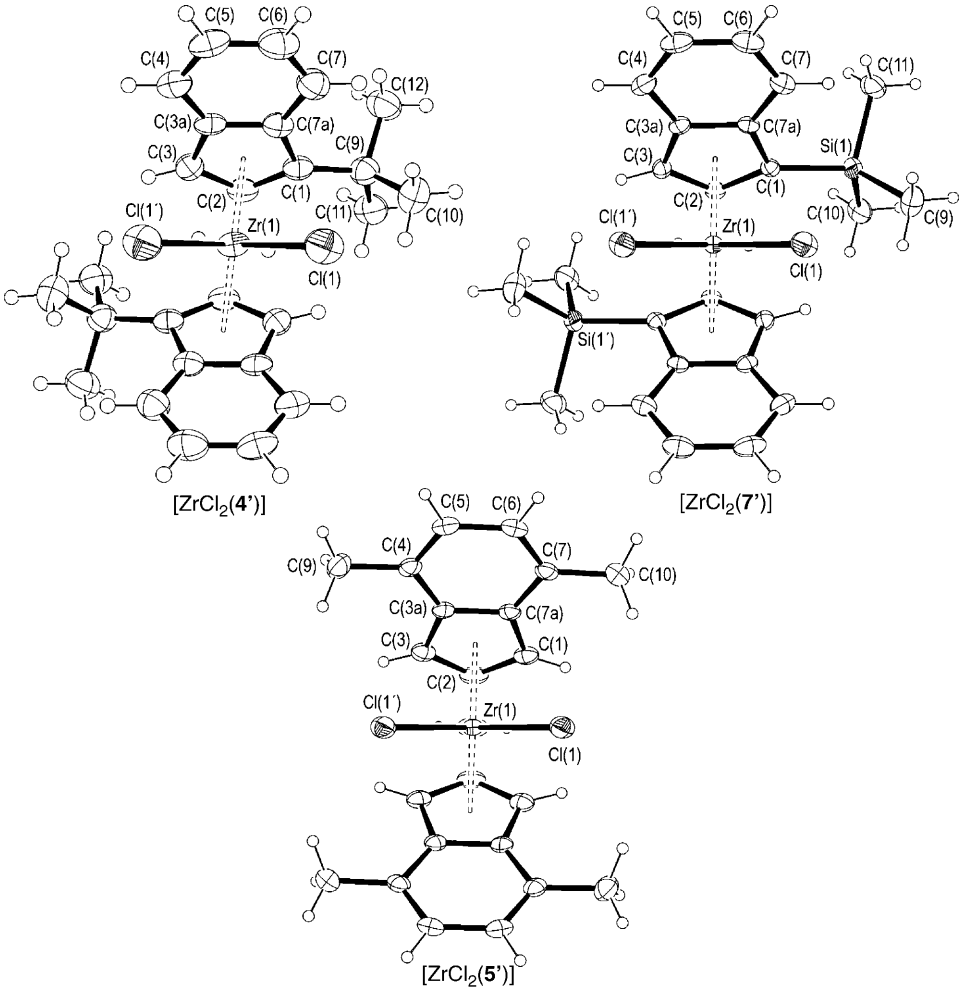


Fig. 6. *ORTEP Views of the methylene-bridged 'zirconocenes' [$ZrCl_2$(**4′**)], [$ZrCl_2$(**7′**)], and [$ZrCl_2$(**5′**)]*. Displacement ellipsoids are drawn at the 30% probability level. H-Atoms have arbitrary radii. The atom numbering of the side chains is arbitrary, the linking methylene being $CH_2$(8).

yl)$_2$}] (bite angle 71.5°) [17] and to the (ethane-1,2-diyl)-bridged complex [$ZnCl_2${*rac*-1,1′-$C_2H_4$(4,7-$Me_2$-1*H*-inden-1-yl)$_2$}] (bite angle 59.9°) [22].

The limited sensitivity of the geometric descriptors to indenyl substitution is further confirmed by the observation that the only noticeable difference between the three $CH_2$-bridged species is the slightly more open $\beta$ angle of the 4,4′,7,7′-tetramethyl substituted compound [$ZrCl_2$(**5′**)] with respect to the 1,1′-disubstituted compounds [$ZrCl_2$(**4′**)] and [$ZrCl_2$(**7′**)]. This small difference appears even more negligible taking into account that the bite angle measured for an individual species can vary by as much as 1.5° depending on which polymorph or particular independent molecule in the asymmetric unit is considered [21]. This considerable dependence of the bite

Table 2. *Selected Bond Lengths* [Å] *and Angles* [°] *of [ZrCl$_2$(**4**′)], [ZrCl$_2$(**7**′)], and [ZrCl$_2$(**5**′)]*[a])

| | [ZrCl$_2$(**4**′)] | [ZrCl$_2$(**7**′)] | [ZrCl$_2$(**5**′)] |
|---|---|---|---|
| Zr(1)–cp(1) | 2.250(3) | 2.2277(16) | 2.2316(10) |
| Zr(1)–Cl(1) | 2.412(2) | 2.4187(10) | 2.4248(6) |
| Zr(1)–C(1) | 2.636(6) | 2.523(2) | 2.4767(19) |
| Zr(1)–C(2) | 2.477(6) | 2.458(2) | 2.454(2) |
| Zr(1)–C(3) | 2.399(6) | 2.457(2) | 2.4639(19) |
| Zr(1)–C(3a) | 2.574(5) | 2.615(3) | 2.6401(19) |
| Zr(1)–C(7a) | 2.682(6) | 2.634(2) | 2.6502(18) |
| C(1)–C(2) | 1.412(8) | 1.438(3) | 1.407(3) |
| C(1)–C(7a) | 1.461(8) | 1.450(3) | 1.434(3) |
| C(2)–C(3) | 1.412(8) | 1.404(3) | 1.410(3) |
| C(2)–C(8) | 1.540(8) | 1.518(3) | 1.514(3) |
| C(3)–C(3a) | 1.432(8) | 1.428(3) | 1.434(3) |
| C(3a)–C(4) | 1.428(8) | 1.424(3) | 1.426(3) |
| C(3a)–C(7a) | 1.409(8) | 1.434(3) | 1.430(3) |
| C(4)–C(5) | 1.351(9) | 1.355(4) | 1.354(3) |
| C(5)–C(6) | 1.376(9) | 1.417(4) | 1.420(3) |
| C(6)–C(7) | 1.369(9) | 1.360(4) | 1.356(3) |
| C(7)–C(7a) | 1.413(8) | 1.421(3) | 1.423(3) |
| C(1)–C(9) | 1.526(8) | | |
| C(1)–Si(1) | | 1.899(2) | |
| C(4)–C(9) | | | 1.500(3) |
| C(7)–C(10) | | | 1.502(3) |
| cp(1)–Zr(1)–cp(1′) | 115.2(2) | 115.56(7) | 115.60(3) |
| cp(1)–Zr(1)–Cl(1) | 107.34(15) | 109.93(6) | 109.07(3) |
| cp(1)–Zr(1)–Cl(1′) | 114.74(15) | 111.55(6) | 111.54(3) |
| Cl(1)–Zr(1)–Cl(1′) | 96.15(11) | 96.77(5) | 98.76(3) |
| C(2)–C(1)–C(7a) | 105.4(5) | 105.55(18) | 108.60(19) |
| C(1)–C(2)–C(3) | 110.1(5) | 109.37(19) | 107.96(18) |
| C(1)–C(2)–C(8) | 129.7(5) | 125.17(18) | 123.73(19) |
| C(3)–C(2)–C(8) | 117.3(5) | 122.12(18) | 124.82(19) |
| C(2)–C(3)–C(3a) | 108.0(5) | 109.01(19) | 108.61(19) |
| C(3)–C(3a)–C(4) | 131.7(6) | 133.5(2) | 132.3(2) |
| C(3)–C(3a)–C(7a) | 107.2(5) | 106.69(19) | 107.10(18) |
| C(4)–C(3a)–C(7a) | 121.1(6) | 119.8(2) | 120.57(18) |
| C(3a)–C(4)–C(5) | 117.9(6) | 119.3(2) | 116.55(19) |
| C(4)–C(5)–C(6) | 121.4(6) | 121.1(2) | 122.75(19) |
| C(5)–C(6)–C(7) | 122.4(7) | 121.4(2) | 122.7(2) |
| C(6)–C(7)–C(7a) | 118.9(6) | 119.6(2) | 116.49(19) |
| C(1)–C(7a)–C(3a) | 109.3(5) | 109.15(19) | 107.29(18) |
| C(1)–C(7a)–C(7) | 132.6(6) | 132.1(2) | 131.8(2) |
| C(3a)–C(7a)–C(7) | 118.1(5) | 118.8(2) | 120.85(18) |
| C(2)–C(8)–C(2′) | 101.8(6) | 101.3(2) | 100.9(2) |
| C(2)–C(1)–C(9) | 130.2(6) | | |
| C(7a)–C(1)–C(9) | 123.1(5) | | |
| C(2)–C(1)–Si(1) | | 129.43(17) | |
| C(7a)–C(1)–Si(1) | | 122.68(16) | |
| C(3a)–C(4)–C(9) | | | 120.5(2) |
| C(5)–C(4)–C(9) | | | 122.9(2) |
| C(6)–C(7)–C(10) | | | 123.4(2) |
| C(7a)–C(7)–C(10) | | | 120.1(2) |

[a]) cp refers to the centroid of the five-membered ring of the organic ligand. Primes refer to symmetry-equivalent atoms ($-x$, $y$, $\frac{1}{2}-z$). For atom numbering, see *Fig. 6*.

Table 3. *Relevant Geometric Parameters of [$ZrCl_2$(**4′**)], [$ZrCl_2$(**7′**)], and [$ZrCl_2$(**5′**)]*[a])

| | [$ZrCl_2$(**4′**)] | [$ZrCl_2$(**7′**)] | [$ZrCl_2$(**5′**)] |
|---|---|---|---|
| $\alpha$ | 115.2 | 115.6 | 115.6 |
| $\beta$ | 74.3 | 75.1 | 76.9 |
| $\phi$ | 101.8 | 101.3 | 100.9 |
| $\delta$ | 82.4 | 84.5 | 83.7 |
| $\Gamma$ | 13.1 | 13.1 | 12.0 |
| $ZrCl_2$–cp | 37.2 | 37.6 | 38.5 |
| bh–cp–cp′–bh′ | 10.7 | 4.6 | −1.2 |
| $\Omega$ | 3.1 | 4.8 | 6.5 |
| $\Delta$ | 0.30 | 0.21 | 0.24 |

[a]) All quantities are given in degrees apart from $\Delta$ [Å]. The angles $\alpha$, $\beta$, $\phi$, $\delta$, and $\gamma$, are defined in *Fig. 7*. cp and $ZrCl_2$ refer to the least-squares planes defined by the five-membered ring and the $ZrCl_2$ atoms, respectively. bh refers to the centroid of the bridge-head atoms (C(3a) and C(7a)). $\Omega$ is the angle between the plane defined by the allylic moiety (C(1), C(2), C(3)) and the least-squares plane defined by the atoms C(1), C(7a), C(3a), and C(3). $\Delta$ is the distance between the perpendicular projection of the heavy atom on the ring least-squares plane and the ring centroid.

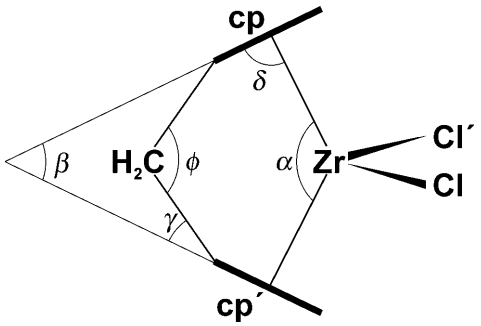


Fig. 7. *Schematic representation of an* 'ansa-*zirconocene' molecule describing the angles listed in* Table 3. $\phi$ is the angle C(2)–C(8)–C(2′), $\delta$ is the angle between the Zr–cp vector and the cp least-squares plane, $\gamma$ is the angle between the C(2)–C(8) vector and the cp least-squares plane, $\beta$ is the angle between the least-squares planes of the two cyclopentadienyl ligands (the 'bite angle'), and $\alpha$ is the angle cp–Zr–cp′. For atom numbering, see *Fig. 6*.

angle on packing interactions is in agreement with the expected low energy associated with the process of ring tilting in metallocenes.

On comparing the 1,1′-di(*tert*-butyl)-substituted compound [$ZrCl_2$(**4′**)] to the 1,1′-bis(trimethylsilyl)-substituted one [$ZrCl_2$(**7′**)], we notice that the *tert*-butyl substituent, being closer to the metal atom, leads to great distortions in the coordination geometry of the bis[1*H*-inden-1-yl] moiety. This effect is recognizable by comparing: *i*) visually the two frontal views shown in *Fig. 6*, *ii*) the 'equivalent' bond distances of C(1) and C(3) from the metal atom (Zr–C(1) *vs.* Zr–C(3): 2.64 *vs.* 2.40 Å in [$ZrCl_2$(**4′**)], 2.52 *vs.* 2.46 Å in [$ZrCl_2$(**7′**)]), *iii*) the 'equivalent' bond angles about the Zr-atom (cp–Zr–Cl *vs.* cp–Zr–Cl′: 107.3 *vs.* 114.7° in [$ZrCl_2$(**4′**)], 109.9 *vs.* 111.6° in [$ZrCl_2$(**7′**)]), and *iv*) the dihedral angles between the $ZrCl_2$ and $Zr(cp)_2$ planes (84.5° in

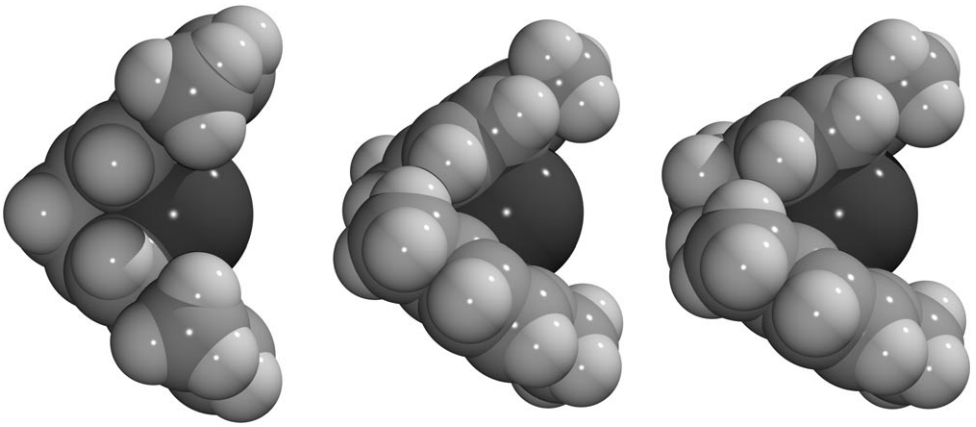


Fig. 8. *Lateral views of the* van der Waals *surfaces of the 2,2′-mehylenebis[4,7-dimethyl-1*H*-inden-1-yl] derivative [ZrCl*$_2$*(***5**′*)], and of the 1,1-methylenebis[4,7-dimethyl-1*H*-inden-1-yl], and 1,1′-(ethane-1,2-diyl)bis[4,7-dimethyl-1*H*-inden-1-yl)-coordinated 'dichlorozirconocene' derivatives.* For clarity, the Cl-atoms are not shown.

[$ZrCl_2$(**4**′)], 88.8° in [$ZrCl_2$(**7**′)]). Moreover, unfavorable steric interactions between the *tert*-butyl substituent and the *ansa* atoms lead to a marked difference in the 'equivalent' bond angles about the bridgehead atom C(2) (C(1)–C(2)–C(8) *vs.* C(3)–C(2)–C(8): 129.7 *vs.* 117.3° in [$ZrCl_2$(**4**′)], 125.2 *vs.* 122.1° in [$ZrCl_2$(**7**′)]) and eventually to a more open arrangement of the two indenyl moieties (note the bh–cp–cp′–bh′ values of 10.7 and 4.6° for [$ZrCl_2$(**4**′)] and [$ZrCl_2$(**7**′)], resp.).

In the achiral compound [$ZrCl_2$(**5**′)], the presence of four methyl substituents in the region directly in front of the $ZrCl_2$ moiety is associated with an increase in the distance of the bridgehead atoms C(3a) and C(7a) from the metal atom (mean value 2.645 Å), leading to a marked ring slippage, as shown by the $\Omega$ value given in *Table 3*.

According to an adaptation by *Schlögl* [23] of the *Cahn–Ingold–Prelog* rules, the stereoisomer of [$ZrCl_2$(**4**′)] and [$ZrCl_2$(**7**′)] represented in *Fig. 6* has the (2*S*,2′*S*) configuration. However, as they crystallize in a centrosymmetric space group, their (2*R*,2′*R*) enantiomers are also present both in solution and in the solid state.

4. *Polymerization of Ethylene* (= *Ethene*). MAO-Activated complexes [$ZrCl_2$(L)] (L = **1**′–**8**′) were tested for ethylene polymerization (MAO = methylaluminoxane). The results are reported in *Table 4*. The polyethylenes (PE) were analyzed by both $^1$H- and $^{13}$C-NMR to determine the end group and branching structures. Assignments were made by using spectra of ethylene/but-1-ene copolymers as reference for ethyl branches and spectra of ethylene/dec-1-ene copolymers as reference for resonances associated with long-chain branches [24]. The amount of ethyl and long-chain branches for 100 C-atoms were calculated from the signals at $\delta$(C) 39.64 and 38.18, respectively, over the sum of all the C-atoms. The branches are of two types: Et branches and branches of 8 or more C-atoms; no branches of intermediate length could be detected. The Et branches arise from chain transfer to ethylene followed by reinsertion of the

Table 4. *Ethylene Homopolymerization*[a])

| Precatalyst (amount [mg]) | Time [min] | Al/Zr [mol/mol] | kg/mmol$_{Zr}$/h | $M_v$[b]) | $T_m$[c]) [°] | Ethenyl end groups [% total end groups] | Ethenylidene end groups [% total end groups] | $P_n$ ($^1$H-NMR)[d]) | Internal ethene-1,2-diyl [% total unsaturations] | Branches ($^{13}$C-NMR) |
|---|---|---|---|---|---|---|---|---|---|---|
| [$ZrCl_2$(**1′**)] (0.3) | 10 | 1000 | 12 | 4500 | 125 | 91.5 | 8.5 | 125 | 6.5 | Et 0.15%, $\geq C_8$ 0.09% |
| [$ZrCl_2$(**2′**)] (0.2) | 23 | 5000 | 472 | 6000 | 120 | 94.1 | 5.9 | 147 | 5.8 | Et 0.29%, $\geq C_8$ 0.16% |
| [$ZrCl_2$(**3′**)] (0.2 | 60 | 500 | 34 | 158700 | 142 | | | | | linear |
| [$ZrCl_2$(**4′**)] (0.2 | 20 | 5000 | 140 | 120100 | 135 | | | | | linear |
| [$ZrCl_2$(**5′**)] (0.5) | 60 | 500 | 25 | 44400 | 129 | 72.5 | 27.5 | 2066 | 53.3 | n.m.[e]) |
| [$ZrCl_2$(**6′**)] (0.5) | 60 | 500 | 15 | 11300 | 123 | 95.9 | 4.1 | 138 | 4.1 | n.m.[e]) |
| [$ZrCl_2$(**7′**)] (0.5) | 60 | 500 | 46 | 45100 | 132 | 100 | 0 | 2131 | 43.4 | n.m.[e]) |
| [$ZrCl_2$(**8′**)] (0.2) | 60 | 500 | 45 | – | – | 100 | 13.2 | 1060 | 13 | n.m.[e]) |

[a]) MAO, 80°, hexane, 9.6 bar ethylene (= ethene). [b]) $M_v$ = viscosity molecular mass. [c]) $T_m$ = melting temperature. [d]) Polymerization degree by $^1$H-NMR. [e]) n.m. = not measured.

polymeryl chain into the Zr–ethyl bond, as shown in *Scheme 18* [25], while the long-chain branches must arise from insertion of ethenyl-terminated ethylene macromers into a growing polyethylene chain, possibly without complete chain desorption from the metal coordination sphere (see *Scheme 19*).

Scheme 18. *Formation of Ethyl Branches on Polymerization of Ethylene*

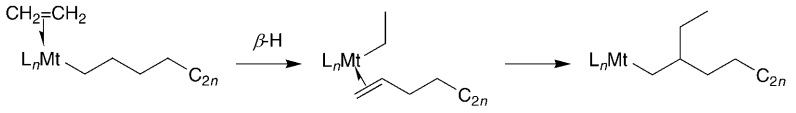


Scheme 19. *Formation of Long-chain Branches on Polymerization of Ethylene*

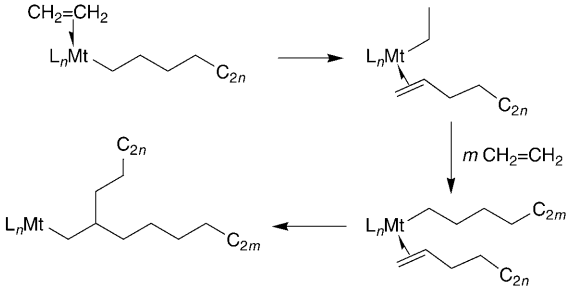


Some of the PE samples are of low molecular mass. $^1$H-NMR allows the identification of three olefinic groups: the largely predominant terminal ethenyl group ($CH_2$=CHCH$_2$, *m* at $\delta$(H) 4.92–5.07; CH$_2$=C*H*CH$_2$, *m* at 5.80–5.90; formed upon $\beta$-H transfer to ethylene), the ethenylidene group ($CH_2$=C(R)–CH$_2$–, *s* at $\delta$(H) 5.73, formed upon $\beta$-H transfer after primary insertion of an $\alpha$-olefin oligomer), and the ethene-1,2-diyl group R–CH=CH–R (*m* at $\delta$(H) 5.44) [18]. The ethene-1,2-diyl group leaves an ambiguity since it could have either (*Z*) or (*E*) configuration, and be either terminal (but-2-enyl end group) or internal. This problem was solved by $^{13}$C-NMR, by comparison with the spectra of (2*Z*)- and (2*E*)-hept-2-ene: the absence of Me resonances at $\delta$(C) 12.5 (2*Z*) or 17.6 (2*E*) and the presence of a single CH$_2$ resonance at $\delta$(C) 32.8, indicates that the ethane-1,2-diyl group is both (*E*) configurated and internal, *i.e.*, R–*C*H$_2$CH=CH*C*H$_2$–R ((2*E*)-hept-2-ene: CH$_2$(4) at $\delta$(C) 32.2; (2*Z*)-hept-2-ene: CH$_2$(4) at $\delta$(C) 26.7). The formation of internal (*E*)-ethene-1,2-diyl groups in metallocene-catalyzed ethylene polymerization can arise from either allylic activation [26] or $\beta$-H transfer following a secondary insertion of an $\alpha$-olefin oligomer. This latter mechanism would be consistent with a unimolecular chain-release process, as already suggested for the case of propylene polymerization with a highly congested catalyst [27]. The only detectable saturated end group is the unbranched alkyl chain.

5. *Polymerization of Propylene* (=*Prop-1-ene*). Both 2,2′-methylenebis[1*H*-inden-1-yl]-coordinated [ZnCl$_2$(**1′**)] and 2,2′-(ethane-1,2-diyl)bis[1*H*-inden-1-yl)-coordinated [ZrCl$_3$(L)] [9] were practically inactive under our conditions for propylene polymerization. All tested catalysts substituted at the indenyl moieties gave atactic polypropylene (a-PP) of low to medium molecular masses. Selected results are shown in *Table 5*. Both

catalyst activity and a-PP molecular mass increase with the size of the substituent at the Cp moieties. As expected, catalyst activity decreases and a-PP molecular mass increases on replacement of Zr by Hf. The 4,7-dimethyl-1*H*-indenyl derivative [$ZrCl_2$(**5**′)] shows a surprisingly high activity.

Table 5. *Propylene Homopolymerization*[a])

| Precatalyst (amount [mg]) | Al/Zr [mol/mol] | kgPP/$mmol_{Mt}$/h | $\bar{M}_v$[b]) | $\bar{P}_N$[c]) |
|---|---|---|---|---|
| [$ZrCl_2$(**1**′)] (2) | 1500 | | – | – |
| [$ZrCl_2$(**2**′)] (5) | 1000 | 2 | – | 26 |
| [$ZrCl_2$(**3**′)] (1) | 3000 | 40 | 18700 | 263 |
| [$ZrCl_2$(**4**′)] (0.2) | 5000 | 73 | 33500 | 430 |
| [$HfMe_2$(**4**′)] (2) | 1000 | 14 | 90200 | ≈1100 |
| [$ZrCl_2$(**5**′)] (0.25) | 3000 | 447 | 20600 | 255 |
| [$ZrCl_2$(**7**′)] (0.5) | 1000 | 284 | 26900 | |
| [$ZrCl_2$(**8**′)] (0.5) | 1000 | 63 | 39300 | 487 |

[a]) 50°, 1 h, 300 g of propylene (= prop-1-ene), MAO co-catalyst. [b]) $\bar{M}_v$ = average viscosity molecular mass, estimated from intrinsic viscosity (THN, 135°). [c]) $\bar{P}_N$ = average polymerization degree by $^1$H-NMR.

*Fig. 9* shows the methyl pentad region of the $^{13}$C-NMR spectrum of two a-PP samples, obtained with the catalysts [$HfMe_2$(**4**′)] and [$ZrCl_2$(**8**′)]. The spectrum shows the lack of enantiofacial preference in propylene insertion. All other a-PP samples show the same or very similar pentad distributions. Chain release occurs by $\beta$-H transfer, as shown by the presence of ethenylidene end groups ($^1$H-NMR), which were used to determine the average polymerization degree, under the assumption that no chain transfer to Al occurs with these catalyst systems.

**Conclusions.** – A one-step, highly atom-economical synthesis of 2,2′-methylenebis[1*H*-indenes] from a variety of substituted 1*H*-indenes was efficiently achieved. The yields of the condensation step were higher with 3-substituted 1*H*-indenes. Double deprotonation with BuLi followed by metallation with $ZrCl_4$ or $HfCl_4$ proceeded in good to high yields, and the diastereoselectivity of metallation was driven by the bulkiness of the substituent at C(1) and C(1′) of the intermediate bis[1*H*-inden-1-yl] anions.

Methylene-bridged '*ansa*-zirconocenes' show a noticeable open arrangement of the bis[1*H*-inden-1-yl] moiety, as measured by the angle between the planes defined by the two $\pi$-ligands (the 'bite angle'). In particular, the 2,2′-methylenebis[4,7-dimethyl-1*H*-inden-1-yl] derivative [$ZrCl_2$(**5**′)] is the most open 'zirconocene' structurally characterized so far. Interestingly, this catalyst shows a very high activity in propylene polymerization.

All the metallocenes tested produced low-molecular-mass, fully atactic polypropylenes. Ethylene could be polymerized with high activities to PE with molecular masses which strongly depended on the substitution of the ligands. In some cases, ethyl and long-chain branches were observed. PE waxes were obtained in quite high yields and a high selectivity for $\alpha$-olefin end groups.

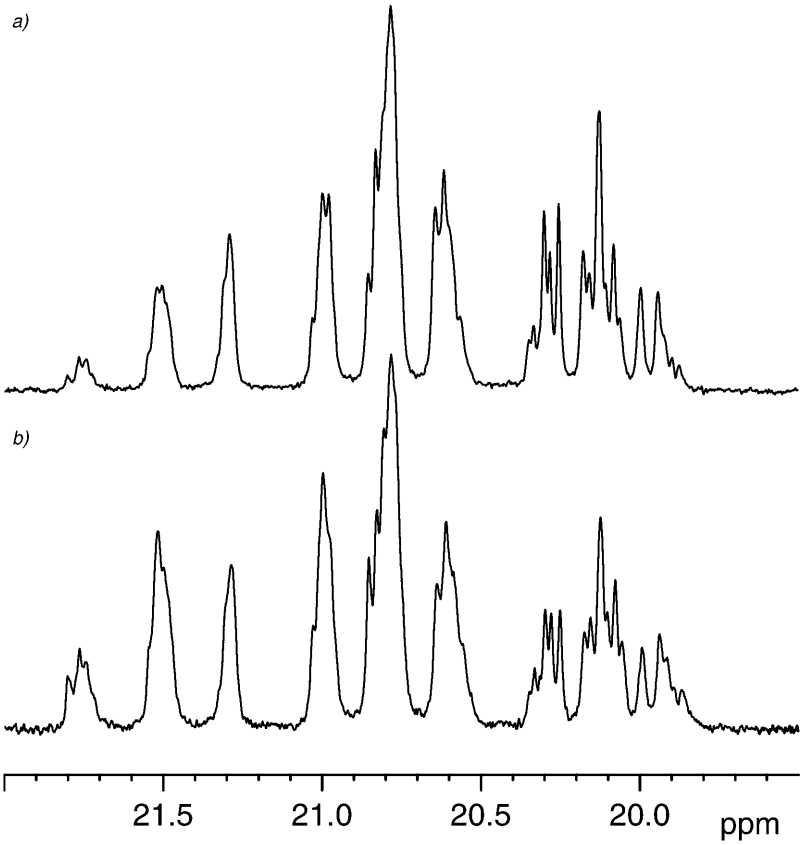


Fig. 9. *Methyl pentad region of the* $^{13}$*C-NMR* ($C_2D_2Cl_4$, 120°) *spectrum of a-PP obtained with the catalyst systems* a) rac-*[ZrCl*$_2$(**8′**)*]/MAO* (liquid propylene, $T_p$ 50°, *mm* = 17.6%, *mr* = 44.2%, *rr* = 38.2%) *and* b) rac-*[HfMe*$_2$(**4′**)*]/MAO* (liquid propylene, $T_p$ 50°, *mm* = 22.1%, *mr* = 50.5%, *rr* = 27.4%).

## Experimental Part

1. *General.* $^1$H-NMR Spectra: $\delta$ in ppm rel. to $CDHCl_2$ ($\delta$ 5.377) or $C_6D_5H$ ($\delta$ 7.15) for $CH_2Cl_2$ or $C_6D_6$ solns. (at r.t.).

2. *Synthesis of the Ligands.* A mixture of formaldehyde (formaline, 37% (wt.) in $H_2O$), 4-toluenesulfonic acid monohydrate ($TSOH \cdot H_2O$), toluene, and the 1*H*-indene was heated to 80° under stirring. The type of indene, amounts of reagents, time of reaction, and yields are specified in *Table 1*. The reaction was quenched with $H_2O/NaHCO_3$ and the org. layer washed with $H_2O$, and evaporated. The crude product crystallized upon standing at r.t., and was then further purified by washing with pentane or MeOH. Similar results were obtained with 1,3-dioxolane as the source of formaldehyde. For example, **1** was obtained with 50% conversion with 1 equiv. of 1,3-dioxolane and TsOH, in toluene after 6 h at 80°. The reaction mixture contained also 10% of the 1*H*-indene dimer.

*2,2′-Methylenebis[3-(*tert*-butyl)-1*H*-indene]* (**4**). $TSOH \cdot H_2O$ (4.1 g, 21.6 mmol), toluene (200 ml), 1,3-dioxolane (*Aldrich*; 7.6 ml, 108.8 mmol), and 3-(*tert*-butyl)-1*H*-indene (19.0 g, 110 mmol) were mixed in this order and then heated to 80° within 20 min and stirred at 80° for 6 h. After cooling to r.t., the mixture was poured onto ice/$NaHCO_3$, the aq. layer washed with $Et_2O$ (2 × 150 ml), and the combined org.

phase dried ($NaSO_4$) and evaporated: red paste (18.6 g) containing 82% of **4** (77% conversion). This paste was taken up in pentane (50 ml), the mixture stirred for 30 min and filtered, the filtrate evaporated, and the residue dried *in vacuo*: 7.0 g (34.8%, purity 97.5% by GC) of **4**. Ochre powder. $^1$H-NMR: *Table 6*.

Table 6. *$^1$H-NMR* ($CDCl_3$, r.t.) *of the Ligand Precursors* **1**–**5**. $\delta$ in ppm.

| | |
|---|---|
| **1** | 7.1–7.5 (*m*, 8 H); 6.65 (*s*, 2 H); 3.72 (*s*, 2 H); 3.40 (*s*, 4 H) |
| **2** | 7.2–7.5 (*m*, 8 H); 3.73 (*s*, 2 H); 3.35 (*s*, 4 H ); 2.29 (*s*, 6 H) |
| **3** | 7.1–7.7 (*m*, 18 H); 3.76 (*s*, 2 H); 3.39 (*s*, 4 H) |
| **4** | 7.1–7.4 (*m*, 6 H); 7.6–7.8 (*d*, 2 H); 4.23 (*s*, 2 H); 3.34 (*s*, 4 H ); 1.58 (*s*, 18 H) |
| **5** | 7.1–6.9 (*m*, 4 H); 6.78 (*s*, 2 H); 3.79 (*s*, 2 H); 3.29 (*s*, 4 H); 2.45 (*s*, 6 H); 2.33 (*s*, 6 H) |

*2,2′-Methylenebis[3-methyl-1*H*-indene]* (**2**). A soln. of 2,2′-methylenebis[1*H*-indene] (**1**; 5.11 g, 91.1% by GC, 19 mmol) in THF (50 ml) in a *Schlenk* tube was cooled to $-40°$, and 1.6M MeLi in $Et_2O$ (27 ml, 42.4 mmol) was added dropwise. The resulting brown soln. was then stirred for 2 h at r.t., and then added dropwise (over 2.5 h) to MeI (2.64 ml, 42 mmol) in THF (100 ml) cooled to $-10°$. After the addition, the mixture was allowed to reach r.t. and stirred overnight. The yellow-brown soln. was quenched with $H_2O$ (100 ml), the aq. layer extracted twice with $Et_2O$, and the combined org. phase dried ($MgSO_4$) and evaporated: 5.61 g (84%, purity 85% by GC) of oily **2** which was analyzed by GC/MS and $^1$H-NMR: *Table 6*.

*2,2′-Methylenebis[1-(trimethylsilyl)-1*H*-indene]* (**7**). A soln. of **1** (6.0 g, purity 77% by GC, 18.9 mmol) in $Et_2O$ (70 ml) was cooled to $-50°$ and treated with 2.5M BuLi in hexane (16 ml, 39.8 mmol). The orange suspension was allowed to reach r.t., stirred for 5 h, and then added to a soln. of $Me_3SiCl$ (5 ml, 39.8 mmol) in $Et_2O$ (30 ml) previously cooled to $-30°$. The yellow suspension was allowed to reach r.t., stirred overnight, then quenched with MeOH, and filtered. The filtrate was evaporated: **7** (8.2 g, purity 71.5% by GC; *meso*/*rac* 1:1). Clear, thick orange oil which was used as such in the zirconation reaction. $^1$H-NMR ($CDCl_3$): 0.03 (*s*, $Me_3Si$); 0.05 (*s*, $Me_3Si$); 3.40 (*s*, 2 H, CHSi); 3.59 (*s*, 2 H, CHSi); 3.85 (*s*, 2 H, $CH_2$ bridge, *rac*); 3.58, 3.66, 3.87, 3.95 (*AB*, $CH_2$ bridge, *meso*); 6.59 (br. *m*, 2 H, H–C(3,3′)); 6.71 (br. *m*, 2 H, H–C(3,3′)); 7.07–7.42 (*m*, 8 arom. H).

*2,2′-Methylenebis[3-methyl-1-(trimethylsilyl)-1*H*-indene]* (**8**). A soln. of **2** (8.05 mmol) in $Et_2O$ (50 ml) was cooled to $-50°$ and treated with 2.5M BuLi in hexane (6.7 ml, 17 mmol). The red-violet suspension was allowed to reach r.t. and then added to a soln. of $Me_3SiCl$ (2.2 ml) in $Et_2O$ (30 ml) previously cooled to $-30°$. The suspension was allowed to reach r.t. (→color fading) and stirred overnight, then quenched with MeOH (→yellow), and filtered. The filtrate was evaporated: **8** (3.55 g, 100%; *meso*/*rac* 1:1). Brown-orange liquid. $^1$H-NMR ($CDCl_3$): −0.12 (*s*, $SiMe_3$); −0.05 (*s*, $SiMe_3$); 1.97 (*m*, Me); 2.13 (*m*, Me); 3.31 (br. *q*, 2 H, CHSi); 3.41 (br. *q*, 2 H, CHSi); 3.76 (*s*, 2 H, $CH_2$ bridge, *rac*); 3.38, 3.46, 3.98, 4.06 (*AB*, 2 H, $CH_2$ bridge, *meso*); 7.03–7.32 (*m*, 8 H, Ar).

3. *Synthesis of the 'Zirconocenes'.* All 'zirconocenes' were prepared in a *Schlenk* tube following standard procedures.

*Dichloro{(1,1′,2,2′,3,3′,3a,3′a,7a,7′a-η)-2,2′-methylenebis[1*H*-inden-1-yl]}zirconium* ([$ZrCl_2$(**1′**)]). To a soln. of **1** (6.9 g, purity 77% by GC, 21.77 mmol) in $Et_2O$ (70 ml), cooled to $-50°$, 2.5M BuLi in hexane (18.3 ml, 45.7 mmol) was added dropwise (→orange slurry). The mixture turned light brown when allowed to warm to r.t., and was stirred for 4 h. After cooling to $-30°$, the mixture was added to a slurry of $ZrCl_4$ (5.0 g, 21.77 mmol) in toluene (50 ml) at $-30°$. Then the mixture was warmed to r.t. (→yellow) and stirred overnight. $Et_2O$ was evaporated from the yellow suspension, which was then filtered over a *G3* frit. The filtrate was discarded, the yellow residue (11.06 g) dried, analyzed by $^1$H-NMR (product and some org. by-products), and extracted with refluxing $CH_2Cl_2$ for 12 h, leaving 6.22 g of crude [$ZrCl_2$(**1′**)] on the filter, containing LiCl. $^1$H-NMR ($CD_2Cl_2$): 4.30 (*s*, 2 H, $CH_2$ bridge); 6.12 (*s*, 4 H, Cp); 7.21–7.31 (*m*, 4 arom. H); 7.49–7.59 (*m*, 4 arom. H).

Since [$ZrCl_2$(**1′**)] has a very low solubility and limited stability in $CH_2Cl_2$, it was not possible to further purify it. Washing with $Et_2O$ and THF to remove LiCl led to partial decomposition. The $CH_2Cl_2$ extract contained some product, starting ligand, and polymeric by-products.

*Dichloro{(1,1′,2,2′,3,3′,3a,3′a,7a,7′a-η)-2,2′-methylenebis[1-methyl-1*H*-inden-1-yl]} zirconium* ([$ZrCl_2$(**2′**)]). To a soln. of **2** (6.5 g, purity 90% by GC, 21.5 mmol) in $Et_2O$ (160 ml), cooled to −20°, 1.6M BuLi in hexane (27 ml, 43.2 mmol) was added dropwise within 15 min. The soln. was allowed to warm to r.t. and stirred for 5 h. The obtained red suspension was then cooled to −80° and added to a slurry of $ZrCl_4$ (5 g, 21.4 mmol) in pentane (160 ml) at −80°. After warming to r.t., the mixture was stirred overnight. The yellow suspension was dried to a free-flowing powder, this powder washed with pentane ($^1$H-NMR: *rac* and *meso* product), transferred into an extraction apparatus and extracted with refluxing $CH_2Cl_2$, (→yellow precipitate in the collecting flask). After the extraction, $CH_2Cl_2$ was concentrated to 20 ml and then the mixture filtered. The residue was washed with $Et_2O$, then pentane, and finally dried: 2.98 g of pure (by $^1$H-NMR) *rac*-[$ZrCl_2$(**2′**)]. Yellow solid. $^1$H-NMR ($CD_2Cl_2$): 2.51 (*s*, 6 H, Me–C(1,1′)); 4.35 (*s*, 2 H, $CH_2$ bridge); 5.95 (br. *s*, 2 H, Cp); 7.19–7.33 (*m*, 4 arom. H); 7.45–7.54 (*m*, 4 arom. H).

*Dimethyl{(1,1′,2,2′,3,3′,3a,3′a,7a,7′a-η)-2,2′-methylenebis[1-methyl-1*H*-inden-1-yl]}zirconium* ([$ZrMe_2$(**2′**)]). To a slurry of [$ZrCl_2$(**2′**)] (0.37 g) in THF (20 ml), cooled to 0°, 1.6M MeLi in $Et_2O$ (0.7 ml, 1.12 mmol) diluted in $Et_2O$ (5 ml) was added (yellow suspension → brick-red soln.). After 2 h at r.t., the mixture was evaporated, the dark red solid extracted with pentane (100 ml) at 30°, the extract concentrated to 10 ml and cooled to −20°, and the obtained precipitate filtered, washed once with a small amount of pentane, and dried *in vacuo*: 0.2 g of *rac*-[$ZrMe_2$(**2′**)]. $^1$H-NMR ($C_6D_6$): −0.72 (*s*, 6 H, $Me_2Zr$); 2.00 (*s*, 6 H, Me–C(1,1′)); 3.27 (*s*, 2 H, $CH_2$ bridge); 5.39 (*s*, 2 H, Cp); 6.91–7.04 (*m*, 4 arom. H); 7.36–7.44 (*m*, 4 arom. H).

*Dichloro{(1,1′,2,2′,3,3′,3a,3′a,7a,7′a-η)-2,2′-methylenebis[1-phenyl-1*H*-inden-1-yl]}zirconium* ([$ZrCl_2$(**3′**)]). To a soln. of **3** (3.5 g, purity 97.3% by GC, 8.59 mmol) in $Et_2O$ (70 ml), cooled to −80°, 2.5M BuLi in hexane (7.5 ml, 18.75 mmol) was added dropwise within 15 min. The soln. was allowed to warm to r.t. and stirred for 6 h. The obtained light brown suspension was then cooled to −80° and added to a slurry of $ZrCl_4$ (2 g, 8.58 mmol) in pentane (80 ml) at −80°. After warming to r.t., the mixture was stirred overnight. The yellow suspension was concentrated to 30 ml and filtered. The solid was dried and then extracted with refluxing $CH_2Cl_2$ until the extract was colorless (→yellow precipitate in the collecting flask). After the extraction, $CH_2Cl_2$ was concentrated to 15 ml, the mixture cooled to −20° overnight, and the precipitate filtered, washed with $CH_2Cl_2$ until the washing turned from brown to yellow, and finally dried: 2.2 g of pure (by $^1$H-NMR) [$ZrCl_2$(**3′**)]. Yellow solid. Additional [$ZrCl_2$(**3′**)] (0.25 g) was recovered from the combined filtrate and washings which were concentrated to 8 ml, cooled to −20° overnight and worked up similarly. Combined yield 51.3%. $^1$H-NMR ($CD_2Cl_2$): 4.74 (*s*, 2 H, $CH_2$ bridge); 5.60 (*m*, 2 H, Cp); 7.23–7.92 (*m*, 8 arom. H).

*Dichloro{(1,1′,2,2′,3,3′,3a,3′a,7a,7′a-η)-2,2′-methylenebis[1-(1,1-dimethylethyl)-1*H*-inden-1-yl]}zirconium* ([$ZrCl_2$(**4′**)]). To a soln. of **4** (3 g, purity 93.1% by GC, 7.83 mmol) in $Et_2O$ (63 ml), cooled to −80°, 1.6M BuLi in hexane (10.6 ml, 16.96 mmol) was added dropwise within 15 min. The soln. was allowed to warm to r.t. and stirred for 5 h. The obtained red suspension was then cooled to −80° and added to a slurry of $ZrCl_4$ (1.96 g, 8.41 mmol) in pentane (63 ml) at −80°. After warming to r.t., the mixture was stirred overnight. The yellow suspension was dried to a free-flowing powder ($^1$H-NMR: only *rac* isomer), and the powder slurried in $CH_2Cl_2$ (100 ml), transferred into an extraction apparatus, and extracted with refluxing $CH_2Cl_2$ for 6 h (→yellow precipitate in the collecting flask). After the extraction, $CH_2Cl_2$ was concentrated to 10 ml and the mixture filtered. The residue was washed with pentane until the washing was colorless, and finally dried: 1.757 g of pure (by $^1$H-NMR) *rac*-[$ZrCl_2$(**4′**)]. Yellow solid. Additional *rac*-[$ZrCl_2$[**4′**)] (0.4 g) was recovered from the filtrate, by recrystallization from toluene and washing with $Et_2O$. Combined yield 55%. $^1$H-NMR ($CD_2Cl_2$): 1.69 (*s*, 18 H, $^t$Bu); 4.90 (*s*, 2 H, $CH_2$ bridge); 6.20 (*m*, 2 H, Cp); 7.17–7.27 (*m*, 4 arom. H); 7.39–7.48 (*m*, 4 arom. H).

*Dimethyl{(1,1′,2,2′,3,3′,3a,3′a,7a,7′a-η)-2,2′-methylenebis[1-(1,1-dimethylethyl)-1*H*-inden-1-yl]hafnium* ([$HfMe_2$(**4′**)]). To a soln. of **4** (1.8 g, purity 97.5% by GC, 4.9 mmol) in $Et_2O$ (30 ml), 1.6M MeLi in $Et_2O$ (12.6 ml, 20.16 mmol) was added dropwise within 5 min at r.t. (exothermic reaction). After 10 min, a white suspension was obtained. Stirring was continued for 2 h. Then the suspension was cooled to −80°, and a slurry of $HfCl_4$ (*Roc-Ric*; 1.62 g, 99.99%, 50.6 mmol) in pentane (30 ml), also cooled to −80°, was added. The mixture was stirred overnight by letting the temp. rise slowly to r.t. in the *Dewar*. The gray suspension was evaporated and the obtained free-flowing powder extracted with pentane (100 ml) in a

*Soxhlet* apparatus for 4.5 h. The extract was dried to a yellow powder (1.46 g) which was taken up in pentane (10 ml), stirred, and filtered. The residue (0.3 g), a light yellow powder, was *rac*-[$HfMe_2$(**4′**)] containing a small amount of impurities. The pentane-soluble fraction was concentrated, treated with $Et_2O$ (2 ml), and cooled to $-20°$. After three days, pure *rac*-[$HfMe_2$(**4′**)] (50 mg) was recovered by filtration. $^1$H-NMR ($C_6D_6$): −0.83 (*s*, 6 H, $Me_2Hf$); 1.47 (*s*, 18 H, $^t$Bu); 3.99 (*s*, 2 H, $CH_2$ bridge); 5.65 (*s*, 2 H, Cp); 6.89–6.96 (*m*, 4 arom. H); 7.31–7.36 (*m*, 2 arom. H); 7.74–7.79 (*m*, 2 H).

*Dichloro{(1,1′,2,2′,3,3′,3a,3′a,7a,7′a-η)-2,2′-methylenebis[4,7-dimethyl-1*H*-inden-1-yl]}zirconium* ([$ZrCl_2$(**5′**)]). To a soln of **5** (2.24 g, purity 89% by GC, 6.66 mmol) in $Et_2O$ (63 ml), cooled to $-80°$, 2.5M BuLi in hexane (6 ml, 15 mmol) was added dropwise within 10 min. The soln. was allowed to warm to r.t. and stirred for 6 h. The obtained pink-red suspension was cooled to $-80°$ and added to a slurry of $ZrCl_4$ (1.6 g, 6.87 mmol) in pentane (63 ml) at $-80°$. After warming to r.t., the mixture was stirred overnight. The yellow-brown suspension was dried to a free-flowing powder and this powder slurried in $CH_2Cl_2$ (100 ml), transferred into an extraction apparatus, and extracted with refluxing $CH_2Cl_2$ for 6 h (→ yellow precipitate in the collecting flask). After the extraction, $CH_2Cl_2$ was concentrated to 20 ml, and the mixture cooled to $-20°$ overnight and finally filtered. The residue was washed with $CH_2Cl_2$ until the washing turned from brown to straw-yellow, and finally dried: 1.215 g of pure (by $^1$H-NMR) [$ZrCl_2$(**5′**)]. Yellow solid. Additional [$ZrCl_2$(**5′**)] (0.734 g) was recovered from the combined filtrate and washings by drying and washing with toluene. Combined yield 63%. $^1$H-NMR ($CD_2Cl_2$): 2.42 (*s*, 12 H, Me); 4.37 (*s*, 2 H, $CH_2$ bridge); 6.03 (*s*, 4 H, Cp); 6.95 (*s*, 4 arom. H).

*Dichloro{(1,1′,2,2′,3,3′,3a,3′a,7a,7′a-η)-2,2′-methylenebis[1-(trimethylsilyl)-1*H*-inden-1-yl]}zirconium* ([$ZrCl_2$(**7′**)]). To a soln. of **7** (8.0 g, purity 71.5% by GC, 14.6 mmol) in $Et_2O$ (70 ml), cooled to $-50°$, 2.5M BuLi in hexane (17.3 ml, 43.2 mmol) was added dropwise within 5 min (orange → red soln.). The soln. was allowed to warm to r.t. and stirred for 5 h. The obtained brick-red suspension was then cooled to $-30°$ and added to a slurry of $ZrCl_4$ (4.8 g, 20.6 mmol) in toluene (50 ml) at $-30°$. After warming to r.t., the yellow mixture was stirred overnight. The yellow suspension was concentrated to remove $Et_2O$ and then filtered. The contents of the toluene soln. were discarded following $^1$H-NMR analysis. The yellow residue on the filter (9.12 g of the target product, containing LiCl) was extracted with refluxing $CH_2Cl_2$ (*Soxhlet*, 7 h). The residue (6.0 g) was pure *rac*-[$ZnCl_2$(**7′**)] containing LiCl. $^1$H-NMR ($CD_2Cl_2$): 0.57 (*s*, 18 H, $Me_3Si$); 4.56 (*s*, 2 H, $CH_2$ bridge); 6.39 (*s*, 2 H, Cp); 7.19–7.33 (*m*, 4 arom. H); 7.48–7.56 (*m*, 2 arom. H); 7.62–7.71 (*m*, 2 arom. H).

The extract (2.75 g) contained some impurities and traces of the *meso* isomer, identified from the diagnostic *q* centered at δ(H) 4.45 ($CH_2$ bridge).

*Dichloro{(1,1′,2,2′,3,3′,3a,3′a,7a,7′a-η)-2,2′-methylenebis[1-methyl-3-(trimethylsilyl)-1*H*-inden-1-yl]}zirconium* ([($ZrCl_2$(**8′**)]). To a soln. of **8** (3.55 g, 8.53 mmol) in $Et_2O$ (50 ml), cooled to $-50°$, 2.5M BuLi in hexane (7.1 ml, 18 mmol) was added dropwise within 5 min (orange → red soln.). The soln. was allowed to warm to r.t. and stirred overnight. The obtained darker red soln. was cooled to $-30°$ and added to a slurry of $ZrCl_4$ (1.98 g, 8.53 mmol) in toluene (50 ml) at $-30°$. After warming to r.t., the brown-violet mixture was stirred overnight. The brown suspension was concentrated to remove $Et_2O$ and then filtered. The residue was discarded following $^1$H-NMR analysis. The toluene soln. was evaporated, the residue washed with $Et_2O$ (50 ml), the mixture filtered, the residue discarded, and the filtrate evaporated again to 3.2 g of a brown product which was then washed with pentane. The residue was dried *in vacuo*: 1.75 g of pure (by $^1$H-NMR) *rac*-[$ZrCl_2$(**8′**)] as the only isomer. $^1$H-NMR ($CD_2Cl_2$): 0.51 (*s*, 18 H, $Me_3Si$); 2.63 (*s*, 6 H, Me–C(1,1′)); 4.56 (*s*, 2 H, $CH_2$ bridge); 7.17–7.32 (*m*, 4 arom. H); 7.43–7.48 (*m*, 2 arom. H); 7.61–7.66 (*m*, 2 arom. H).

4. *X-Ray Diffraction Structural Analysis.* Suitable crystals of [$ZrCl_2$(**4′**)], [$ZrCl_2$(**5′**)], and [$ZrCl_2$(**7′**)], obtained by cooling conc. solns. in $CH_2Cl_2$, were mounted in air on a glass fiber tip which was subsequently fixed onto a goniometer head. Single-crystal X-ray diffraction data were collected at r.t. on a *Siemens-SMART-CCD* area detector diffractometer for [$ZrCl_2$(**7′**)] and on an *Enraf-Nonius-CAD-4* diffractometer for [$ZrCl_2$(**4′**)] and [$ZrCl_2$(**5′**)], with graphite-monochromatized Mo$K_\alpha$ radiation (λ 0.71073 Å). For [$ZrCl_2$(**7′**)], unit-cell parameters were initially obtained from *ca.* 50 reflections taken from 45 frames collected in three different ω regions, and eventually refined against 7182 reflections, while for [$ZrCl_2$(**4′**)] and [$ZrCl_2$(**5′**)], the setting angles of 25 randomly distributed intense reflections with $10° < \theta < 14°$ were processed by least-squares fitting. For [$ZrCl_2$(**7′**)], a full sphere of reciprocal space was scanned by 0.3° ω

steps, collecting 2400 frames each at 30-s exposure and keeping the detector at 5.0 cm from the sample. Intensity decay was monitored by recollecting the initial 100 frames at the end of data collection and analyzing the duplicate reflections. The collected frames were processed for integration, and an empirical absorption correction was made on the basis of 8896 symmetry-equivalent reflection intensities (SADABS [28]; average redundancy: 4.75).

For [$ZrCl_2$(**4′**)] and [$ZrCl_2$(**5′**)] data collection was performed by the $\omega$ scan method with variable scan speed (maximum time per reflection, 90 and 60 s, resp.) and variable scan range ($1.80+0.35\tan\theta$ and $1.00+0.35\tan\theta$ degrees, resp.). Crystal stability under diffraction was checked by monitoring three standard reflections every 180 min. For [$ZrCl_2$(**4′**)], due to crystal decay, the fraction of unique reflections measured out to 23° is only 0.75. The measured intensities were corrected for *Lorentz*, polarization, decay, and background effects and reduced to $F_o^2$. An empirical absorption correction was applied by using $\psi$ scans of three suitable reflections having $\chi$ values close to 90° [29]. Crystal data and data collection parameters are summarized in *Table 7*.

Table 7. *Summary of Crystallographic Data of [$ZrCl_2$(**4′**)],[$ZrCl_2$(**5′**)], and [$ZrCl_2$(**7′**)]*

| | [$ZrCl_2$(**4′**)] | [$ZrCl_2$(**5′**)] | [$ZrCl_2$(**7′**)] |
|---|---|---|---|
| Formula | $C_{27}H_{30}Cl_2Zr$ | $C_{23}H_{22}Cl_2Zr$ | $C_{25}H_{30}Cl_2Si_2Zr$ |
| $M_r$ | 516.63 | 460.53 | 548.79 |
| Crystal system | monoclinic | monoclinic | monoclinic |
| Space group | *C*2/*c* (No.15) | *C*2/*c* (No.15) | *C*2/*c* (No.15) |
| *a* [Å] | 19.450(11) | 15.875(3) | 20.324(11) |
| *b* [Å] | 10.676(3) | 9.360(1) | 10.234(5) |
| *c* [Å] | 12.505(6) | 13.870(3) | 13.166(7) |
| $\beta$ [°] | 113.69(5) | 107.50(1) | 113.34(1) |
| *V* [Å$^3$] | 2377.8(19) | 1965.6(6) | 2514(2) |
| *Z* | 4 | 4 | 4 |
| *F*(000) | 1064 | 936 | 1128 |
| Density [g cm$^{-3}$] | 1.443 | 1.556 | 1.450 |
| Absorption coefficient [mm$^{-1}$] | 0.70 | 0.83 | 0.76 |
| Diffractometer | *Enraf-Nonius CAD-4* | *Enraf-Nonius CAD-4* | *Siemens SMART* |
| $\theta$ range [°] | $3.1\le\theta\le23.0$ | $3.1\le\theta\le26.0$ | $2.2\le\theta\le27.1$ |
| Index ranges | $-21\le h\le11$ | $-13\le h\le19$ | $-25\le h\le25$ |
| | $0\le k\le11$ | $0\le k\le11$ | $-12\le k\le12$ |
| | $-13\le l\le13$ | $-14\le l\le17$ | $-16\le l\le16$ |
| Intensity decay [%] | 14 | none | 4 |
| Absorption correction | $\psi$ scan | $\psi$ scan | SADABS |
| Min transmission factor | 0.62 | 0.92 | 0.90 |
| Measured reflections | 1645 | 1925 | 12608 |
| Independent reflections | 1645 | 1925 | 2584 |
| $R_{int}$, $R_\sigma$ [a]) | –, 0.050 | –, 0.022 | 0.037, 0.036 |
| Reflections with $I>2\sigma(I)$ | 1240 | 1660 | 2086 |
| Data/parameters | 1240 / 137 | 1660 / 119 | 2584 / 137 |
| Weights (*a*, *b*)[b]) | 0.085, 0 | 0.028, 0.87 | 0.040, 0 |
| Goodness-of-fit $S(F^2)$[c]) | 1.07 | 1.12 | 1.00 |
| $R(F)$, $I>2\sigma(I)$[d]) | 0.045 | 0.021 | 0.029 |
| $wR(F^2)$, all data[e]) | 0.085 | 0.052 | 0.068 |
| Largest difference peak and hole [e Å$^{-3}$] | 0.80, −0.85 | 0.22, −0.26 | 0.35, −0.42 |

[a]) $R_{int}=\Sigma|F_o^2-F_{mean}^2|/\Sigma|F_o^2|$; $R_\sigma=\Sigma|\sigma(F_o^2)|/\Sigma|F_o^2$ [b]) $w=1/[\sigma^2(F_o^2)+(aP)^2+bP]$, where $P=(F_o^2+2F_c^2)/3$. [c]) $S=[\Sigma w(F_o^2-F_c^2)^2/(n-p)]^{1/2}$, where *n* is the number of reflections and *p* is the number of refined parameters. [d]) $R(F)=\Sigma||F_o|-|F_c||/\Sigma|F_o$ [e]) $wR(F^2)=[\Sigma w(F_o^2-F_c^2)^2/\Sigma wF_o^4]^{1/2}$.

The structures were solved by direct methods [30] and subsequent *Fourier* synthesis, and they were refined by full-matrix least-squares on $F^2$ [31] by using all reflections for [$ZrCl_2$(**7′**)], and reflections with $I > 2\sigma(I)$ for [$ZrCl_2$(**4′**)] and [$ZrCl_2$(**5′**)]. Scattering factors for neutral atoms and anomalous dispersion corrections were taken from the internal library of SHELX97 [31]. Weights were assigned to individual observations according to the formula $w = 1/[\sigma^2(F_o^2) + (aP)^2 + bP]$, where $P = (F_o^2 + 2F_c^2)/3$; $a$ and $b$ were chosen to give a flat analysis of variance in terms of $F_o^2$. Anisotropic displacement parameters were assigned to all non-H-atoms. H-Atoms were placed in idealized position and refined riding on their parent atom with an isotropic displacement parameter 1.2 times that of the parent C-atom (AFIX 23, 43, and 133 in SHELX97 [21]). The final difference electron density maps showed no features of chemical significance, with the largest peaks lying close to the metal atoms. Final conventional agreement indexes and other structure refinement parameters are listed in *Table 7*.

CCDC-290783–290785 contain the supplementary crystallographic data for this paper. These data can be obtained free of charge *via* http://www.ccdc.cam.ac.uk/data_request/cif. from the *Cambridge Crystallographic Data Centre*.

5. *Polymerizations.* Polymerization-grade propylene, ethylene, and hexane were received directly from the *Montell Ferrara* plant. MAO was a commercial product (*Crompton*; 10% *w*/*w* in toluene) which was used as received.

*Co-catalysts.* Methylalumoxane (MAO): the commercial 10% toluene solution (1.7M; *Crompton*) was used as such. Alternatively, MAO was dried *in vacuo* to a free-flowing powder (residual $AlMe_3$, *ca.* 3–5 mol-%). The catalyst mixture was prepared by adding the desired amount of the metallocene to the proper amount of the MAO soln., obtaining a soln. which was stirred for 10 min at r.t. and then injected into the autoclave at the polymerization temp. in the presence of the monomer.

*Ethylene Polymerizations.* Under ethylene purge, technical hexane (513 ml) and $Al^iBu_3$ (1 mmol) were charged in a 1-l stainless-steel autoclave, previously thermostatted with $H_2O$/steam and purified by purging with ethylene at 80°. The temp. was brought to 80°, and the reactor was vented to remove residual $N_2$ and then pressurized with ethylene up to 9.5 bar-g. The catalyst/co-catalyst mixture was injected with ethylene overpressure, and the ethylene partial pressure was stabilized to 9.6 bar-a, ($P_{tot}$ 11 bar-a). The test was carried out at 80°, 1 h, by maintaining a constant ethylene partial pressure. After degassing unreacted ethylene, the polymer was isolated by filtration and dried in a vacuum oven at 60°.

*Propylene Polymerizations.* Propylene was charged at r.t. in a 1-l or 4.25-l jacketed stainless-steel autoclave, equipped with a magnetically driven stirrer and a 35-ml stainless-steel vial, connected to a thermostat for temp. control, previously purified by washing with a $Al^iBu_3$ soln. in hexanes and dried at 50° in a stream of propylene. $Al^iBu_3$ (1 mmol in hexane) was added as scavenger before the monomer. The autoclave was then thermostatted at 2° below the polymerization temp., and then the toluene soln. containing the catalyst/co-catalyst mixture was injected in the autoclave by means of $N_2$ pressure through the stainless-steel vial, the temp. rapidly raised to the polymerization temp., and the polymerization carried out at constant temp. for 1 h. The polymerizations were stopped with CO, the unreacted monomers vented, and the polymer dried in a vacuum oven at 60°.

## REFERENCES

[1] R. L. Halterman, in 'Metallocenes. Synthesis, Reactivity, Applications', Eds. A. Togni and R. L. Halterman, Wiley-VCH, Weinheim, 1998, Vol. 1, p. 455.

[2] X. Zhang, Q. Zhu, I. A. Guzei, R. F. Jordan, *J. Am. Chem. Soc.* **2000**, *122*, 8093; E. Royo, H.-R. H. Damrau, S. Obert, F. Schaper, A. Weeber, H.-H. Brintzinger, *Organometallics* **2001**, *20*, 5258; H. Gregorius, C. Süling, W. Bidell, H.-H. Brintzinger, H.-R. H. Damrau, A. Weeber, to *Basell*, Int. Pat. Appl. WO 03/046023.

[3] M. H. Nantz, S. R. Hitchcock, S. C. Sutton, M. D. Smith, *Organometallics* **1993**, *12*, 5012.

[4] S. R. Hitchcock, J. J. Situ, J. A. Covel, M. M. Olmstead, M. H. Nantz, *Organometallics* **1995**, *14*, 3732.

[5] H. Palandoken, J. K. Wyatt, S. R. Hitchcock, M. M. Olmstead, M. H. Nantz, *J. Organomet. Chem.* **1999**, *579*, 338.

[6] R. L. Halterman, Z. Chen, M. A. Khan, *Organometallics* **1996**, *15*, 3957.
[7] L. Cavallo, G. Guerra, M. Vacatello, P. Corradini, *Macromolecules* **1991**, *24*, 1784; G. Guerra, L. Cavallo, G. Moscardi, M. Vacatello, P. Corradini, *J. Am. Chem. Soc.* **1994**, *116*, 2988; G. Guerra, L. Cavallo, G. Moscardi, M. Vacatello, P. Corradini, *Macromolecules* **1996**, *29*, 4834; G. Guerra, P. Longo, L. Cavallo, P. Corradini, L. Resconi, *J. Am. Chem. Soc.* **1997**, *119*, 4394.
[8] H. Palandoken, W. T. McMillen, M. H. Nantz, *Org. Prep. Proced. Int.* **1996**, *28*, 702.
[9] C. J. Schaverien, R. Ernst, J.-D. van Loon, T. Dall'Occo, to *Montell*, Eur. Pat. Appl. 941 997, 1999; T. Dall'Occo, G. Baruzzi, C. J. Schaverien, to *Montell*, Eur. Pat. Appl. 942 011, 1999; C. J. Schaverien, R. Ernst, P. Schut, T. Dall'Occo, *Organometallics* **2001**, *20*, 3436.
[10] J. A. M. van Beek, J. G. de Vries, H. J. Arts, R. Pensad, G. H. J. van Doremaele, to *DSM*, Int. Pat. Appl. WO94/11406, 1994.
[11] N. Yabunouchi, K. Yokota, M. Watanabe, T. Okamoto, N. Tani, to *Idemitsu Kosan*, Eur. Pat. Appl. 721 954, 1995.
[12] M. N. Herzog, J. C. W. Chien, M. D. Rausch, *J. Organomet. Chem.* **2002**, *654*, 29.
[13] L. Resconi, to *Montell*, Int. Pat. Appl. WO 00/29415; L. Resconi, *Polymer Preprints* **2002**, *43*, 303.
[14] E. Arundale, L. A. Mikeska, *Chem. Rev.* **1952**, *51*, 505.
[15] C. W. Roberts, in 'Friedel-Crafts and Related Reactions', Ed. G. A. Olah, Interscience, New York, 1964, Chapt. XXVII, p. 1192.
[16] L. Cedheim, L. Eberson, *Synthesis* **1973**, *3*, 159.
[17] D. Balboni, I. Camurati, G. Prini, L. Resconi, S. Galli, P. Mercandelli, A. Sironi, *Inorg. Chem.* **2001**, *40*, 6588.
[18] V. A. Dang, L.-C. Yu, D. Balboni, T. Dall'Occo, L. Resconi, P. Mercandelli, M. Moret, A. Sironi, *Organometallics* **1999**, *18*, 3781.
[19] W.-L. Nie, G. Erker, G. Kehr, R. Fröhlich, *Angew. Chem., Int. Ed.* **2004**, *43*, 310.
[20] M. E. Huttenloch, B. Dorer, U. Rief, M.-H. Prosenc, K. Schmidt, H.-H. Brintzinger, *J. Organomet. Chem.* **1997**, *541*, 219.
[21] CSD version 5.26 (November 2004); F. H. Allen, *Acta Crystallogr., Sect. B: Struct. Sci.* **2002**, *58*, 380.
[22] L. Resconi, F. Piemontesi, I. Camurati, D. Balboni, A. Sironi, M. Moret, H. Rychlicki, R. Zeigler, *Organometallics* **1996**, *15*, 5046.
[23] K. Schlögl, *Top. Stereochem.* **1967**, *1*, 39.
[24] I. Camurati, B. Cavicchi, T. Dall'Occo, F. Piemontesi. *Macromol. Chem. Phys.* **2001**, *202*, 701.
[25] L. Izzo, L. Caporaso, G. Senatore, L. Oliva, *Macromolecules* **1999**, *32*, 6913; G. Melillo, L. Izzo, M. Zinna, C. Tedesco, L. Oliva, *Macromolecules* **2002**, *35*, 9256; L. Izzo, F. De Riccardis, C. Alfano, L. Caporaso, L. Oliva, *Macromolecules* **2001**, *34*, 2.
[26] F. J. Karol, S. Kao, E. P. Wasserman, R. C. Brady, *New J. Chem.* **1997**, *21*, 797; E. Wasserman, E. Hsi, W.-T. Young, *Polym. Prepr. (Am. Chem. Soc., Div. Polym. Chem.)* **1998**, *39*, 425.
[27] L. Resconi, I. Camurati, O. Sudmeijer *Top. Catal.* **1999**, *7*, 145.
[28] G. M. Sheldrick, 'SADABS. Program for Empirical Absorption Correction', Universität Göttingen, Göttingen, 1996.
[29] A. C. T. North, D. C. Phillips, F. S. Mathews, *Acta Crystallogr., Sect. A: Found. Crystallogr.* **1968**, *24*, 351.
[30] A. Altomare, M. C. Burla, M. Camalli, G. L. Cascarano, C. Giacovazzo, A. Guagliardi, A. G. G. Moliterni, G. Polidori, R. Spagna, *J. Appl. Crystallogr.* **1999**, *32*, 115.
[31] G. M. Sheldrick, 'SHELX97. Program for Crystal Structure Refinement', Universität Göttingen, Göttingen, 1997.

*Received January 2, 2006*